APPROVED FOR PUBLIC RELEASE
DISTRIBUTION UNLIMITED

TECHNICAL NOTE 73-1

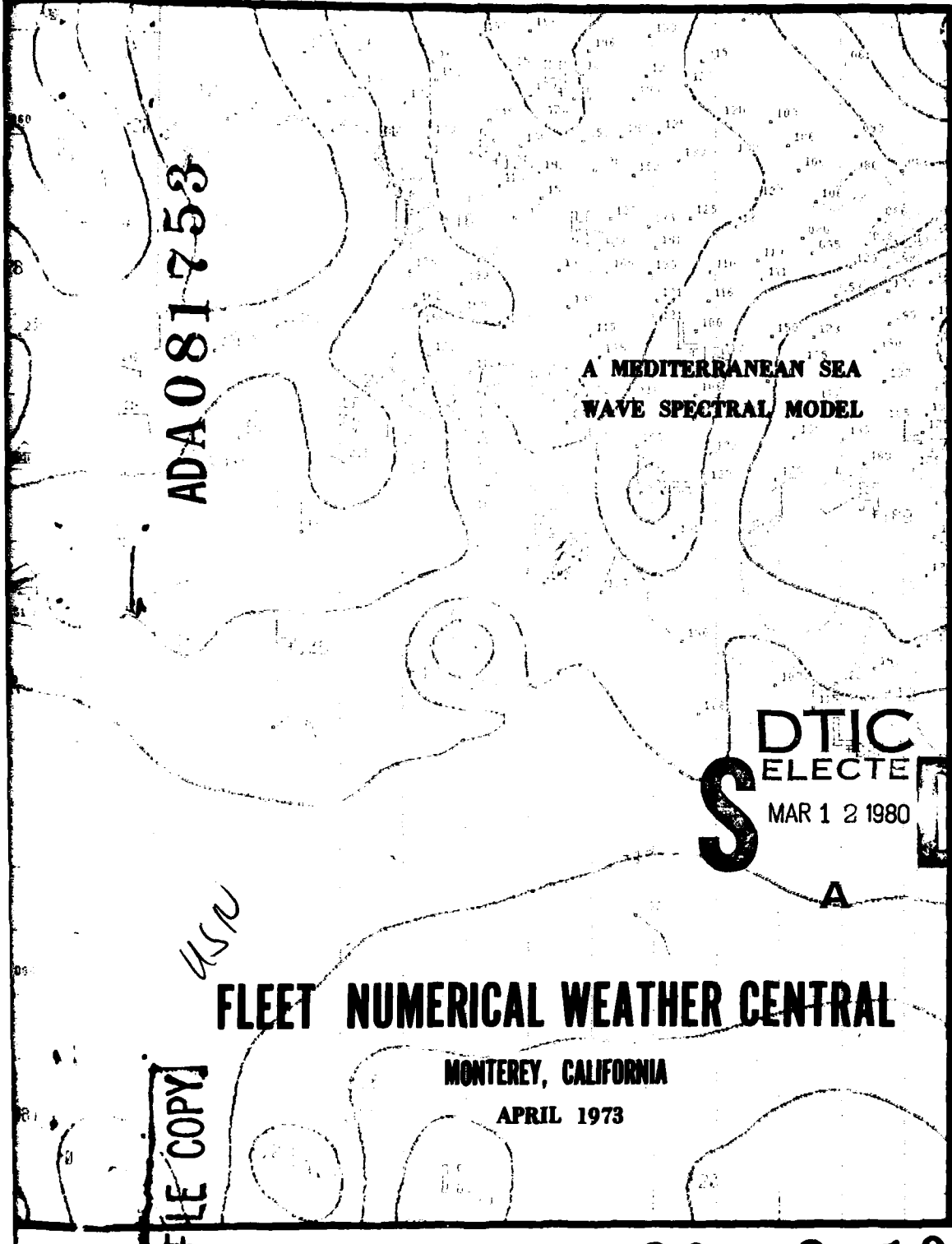

AD A081753

A MEDITERRANEAN SEA WAVE SPECTRAL MODEL

DTIC
ELECTE
MAR 1 2 1980
S D
A

USN

FLEET NUMERICAL WEATHER CENTRAL

MONTEREY, CALIFORNIA

APRIL 1973

DDC FILE COPY

JUL 1 8 1975

80 3 10 074

THIS PAGE IS BEST QUALITY PRACTICABLE
FROM COPY FURNISHED TO DDC

A MEDITERRANEAN SEA WAVE SPECTRAL MODEL

Technical Note No. 73-1

April 1973

by

Sheldon M. Lazanoff
U. S. Naval Oceanographic Office

Norman M. Stevenson
Fleet Numerical Weather Central

Vincent J. Cardone
New York University

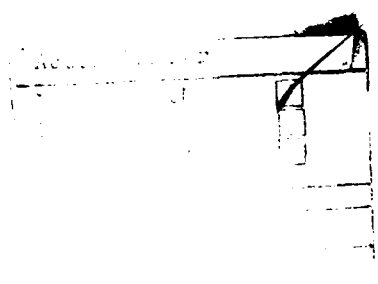

A

FOREWARD

The spectral sea/swell analysis and forecast model described in this technical note is the first to be adapted for real-time use. The program has been running twice daily in the FNWC operational program stream since April 1972. It was developed through the cooperative efforts of the Naval Oceanographic Office, New York University, and Fleet Numerical Weather Central.

In working with any spectral model, verification is always a major problem. Spectral data are quite scarce; calibration and tuning, etc., are very difficult. Fortunately, in this case, we had the services of the Naval Oceanographic Office representative to FNWC, who arranged the joint verification project reported here.

Future plans for this model include evaluation of Environmental Prediction Research Facility's (EPRF) Fields by Information Blending (FIB) wind analysis of the Mediterranean "window" as input, as soon as available.

Reviewed and approved 1 March 1973.

W. S. HOUSTON, Jr.
Captain, U. S.Navy
Commanding Officer
Fleet Numerical Weather Central

TABLE OF CONTENTS

LIST OF FIGURES AND TABLES

Tables

LIST OF SYMBOLS

$A[f,u(t,\vec{x})]$	Phillips resonance growth mechanism
A_m	π
A_p	constant determined by Phillips
A^*	empirical term directly proportional to wave number and inversely proportional to water density and the square of gravity
$B[f,u(t,\vec{x})]$	Miles instability term
C	phase velocity
E_{TOTAL}	total wave energy at a grid point
$F(\omega, \theta, U)$	directional spectra
$\bar{H}_{1/3}$	significant wave height
L	wave length
$S(f,t,\vec{x})$	spectral density as a function of frequency, time and distance
$S_D(f_i,\theta_i)$	spectral component after dissipation
$S_o(f_i,\theta_i)$	spectral component before dissipation
U	wind speed
U^*	wind friction velocity
U'	mean wind profile slope
U''	mean wind profile curvature
Z	elevation
Z_m	matched layer where wind speed and phase are equal
Z_o	roughness parameter
c	constant (690 for ft^2)

f	wave frequency
f_i	center frequency of spectral component
g	gravitational attraction of earth
k	wave number
k_o	von Karman constant
$k(\theta_1)$	constant for given wind direction θ_1
t	time
$\vec{x}$	wave direction
u	wave velocity
Γ^2	constant
α	constant ($8.1 * 10^{-3}$)
β	constant (0.74)
ω	radian frequency
ω_o	directly proportional to g and inversely proportional to wind speed at 19.5 meters
ρ_a	density of air
ρ_w	density of water
π	pi
τ_o	surface stress
θ	angle between wind and wave direction
θ_i	center direction of spectral component

Abstract

An operational Mediterranean wave spectral model has been developed through the cooperative efforts of the U.S. Naval Oceanographic Office (NAVOCEANO), Fleet Numerical Weather Central (FNWC) and New York University (NYU). Since April 1972, the model has been operating in a real-time environment (analyses/prognoses to 48 hours). The model is a modified version of the original NYU North Atlantic wave model and has two main parts: (1) wave energy growth based on a modified version of the Miles-Phillips growth mechanism and dissipation at individual grid points and (2) wave energy propagation from grid point to grid point. The Mediterranean wave model uses a conic conformal grid, permitting the assumption of equal spacing between grid points. There are 455 sea points with a mesh length of 67 km.

The wave model driving force is a modified version of the FNWC Marine Wind model which has a mesh length of approximately 370 kms. For use in the Mediterranean, the winds are interpolated between Marine Wind field grid points. At analysis (or pre-analysis)times, wind reports from synoptic ship files are reanalyzed in the Mediterranean wind program so that local wind phenomena, such as "mistrals," are included in the wind field.

The Mediterranean wind and wave model was evaluated with ship reports, one wave buoy and an airborne wave laser.

The wave computations appear to be as good as the wind input allows.

The on-time analyses and 24-hour forecasts of wave heights are transmitted to Fleet Weather Central, Rota, Spain.

1. Introduction

A Mediterranean (Med) Sea wave spectral forecasting model has been developed through the cooperative efforts of the U.S. Naval Oceanographic Office (NAVOCEANO), Fleet Numerical Weather Central (FNWC) and New York University (NYU). Although various wave spectral models have been in existence for several years, none of the models have been used for wave forecasting on an operational basis primarily due to computer memory and time requirements. Environmental facilities were constrained to developmental spectral modeling and hindcasting projects. Thus, the Med wave model is the first operational wave spectral forecasting model.

The Med wave model is a direct descendant of the original NYU North Atlantic model (Baer, 1962), which has been used several times for hindcasting projects, including a six-week project conducted by the NAVOCEANO representative at FNWC during the summer of 1971. At the completion of this NAVOCEANO study, it was apparent that the North Atlantic model could be adapted as a wave forecasting model. The only serious limitation of this model was its grid system, a Lambert Conformal Grid with a mesh length of 200 kilometers. Since the Lambert Conformal Grid causes large distortions over great distances, it was decided to limit the operational use of this model to small geographical areas such as the Mediterranean and South China Sea.

2. Wave Theory

There are two parts to the basic wave program: (a) growth at each grid point and (b) propagation from grid point to grid point. The wave model treats these two factors independently.

a. Wave Growth

The scheme for computing the growth of the wave energy is based on the work of Inoue (1967). Inoue, under the guidance of Professor Willard J. Pierson, combined and modified the Miles and Phillips growth mechanisms for practical application to wave forecasting. Although Inoue has described this mechanism in great detail, the highlights of his work as related to the Mediterranean Sea will be briefly described in the following paragraphs.

The Miles instability theory (1957) stated that the mean rate of energy transferred from the parallel shear flow to the surface wave is proportional to the curvature of the wind profile and inversely proportional to the slope of the wind profile at the height where the mean wind velocity is the same as the phase speed of the wave component. This theory was originally proposed to overcome the sheltering coefficient difficulties encountered by Jeffries in 1926. Jeffries introduced the sheltering coefficient to improve the Helmholtz instability theory (as described by Lamb, 1932) which required stronger winds than actually observed to generate waves. The sheltering coefficient tried to describe empirically the pressure difference distribution that occurs when a wind passes over a wave,

i.e., high pressure on the windward side and lower pressure on the leeward side. Jeffries' results were an order of magnitude too large. One problem with the sheltering concept is that it will not work in calm seas and, thus, must assume the presence of existing waves.

The Phillips theory essentially stated that a resonance between the air-sea system could occur when a component of the surface pressure distribution moved at the same speed as a free surface wave of the same wave number (where the wave number, k, is equal to $2\pi/L$, and L is equal to wave length). Unlike prior growth theories, this theory can be applied to a calm sea surface. Miles developed a combined resonance-instability model in 1960. Snyder and Cox (1966), using a wave recorder towed by a boat, and Barnett and Wilkerson (1967), using an airborne wave recorder, showed that the wind waves were affected by both mechanisms. Inoue then combined the work of Miles and the more recent efforts of Phillips, (1966). One of the important results of this work is that when the sea starts growing from a calm condition, the resonance mechanism predominates and later, after the wind has been blowing for a given time, the instability mechanism takes over. The resonance mechanism leads to a linear growth as a function of time while the instability mechanism leads to exponential growth, as shown in Figure 1. Cardone (1969) claims that the resonance term contributes only a small part of the energy to

the waves and its chief function is to trigger growth by the instability mechanism.

Neglecting non-linear effects, the spectral components can be initially expressed as

$$\frac{d}{dt} S(f,t,\vec{x}) = A[f,u(t,\vec{x})] + B(f,u(t,\vec{x})] \cdot S(f,t,\vec{x}) \qquad (1)$$

where $A[f,u(t,\vec{x})]$ is the resonance growth mechanism,

$B[f,u(t,\vec{x})] \cdot S(f,t,\vec{x})$ is the Miles instability term,

$S(f,t,\vec{x})$ is the spectral density, and

f is the wave frequency, t is time, $\vec{x}$ is wave direction.

Inoue showed that A(f,u) could be expressed, for the North Atlantic, as

$$\int_{-\pi/2}^{\pi/2} \frac{A^*(\omega)^{5.25}\, U^{2.25}}{[1/4\ (\frac{\omega}{U})^2 + (k \sin\theta)^2][1/9\ (\frac{\omega}{U})^{2.5} + (k\cos\theta - \frac{\omega}{U})^2]}\, d\theta \qquad (2)$$

where $\omega = 2\pi f$,

U = the wind speed at a certain anemometer height (NYU uses 19.5 meters as this is the average anemometer height of the weather ships),

$k = \omega^2/g$ and g is the gravitational acceleration,

A^* is directly proportional to k and inversely proportional to the water density and the square of gravity.

A^* was at first determined from observational data and then modified as the original NYU wave programs were used for hindcasting. A^* is a combination of all the constants as well as

some empirical calculations. Inoue used the value of 9.84 * 10^{-15} for A*. This value was calculated from the Snyder and Cox experiment. Inoue tried to detect the A growth term from spectra calculated from British weather ships and Argus Island Tower data but was unable to reach any definite conclusions. He suggested that the value shown in equation (2) be used and that this growth value be subtracted from observational data to determine the (B•S) term.

Before describing the B term, several other relationships need to be introduced. The first relationship is one which describes the wind profile above the sea surface and is expressed by

$$U(Z) - C/\cos\theta = U^*/k_o \ln (Z/Z_m) \tag{3}$$

where U^* is the frictional velocity equal to $\sqrt{\tau_o/\rho_a}$ and

τ_o is the surface stress and

ρ_a is the atmospheric pressure,

k_o is a von Karman constant,

C is the phase velocity

Z_m is the matched layer where the wind speed and phase speed are the same [$U(Z_m) \cos\theta = C$).

By combining several terms in equation (3), a roughness parameter Z_o can be expressed by

$$Z_o = A_m \exp\left\{\frac{-k_o C}{U^* \cos\theta}\right\} \tag{4}$$

Several empirical relationships have been derived which describe the relationship between Z_o and U^*. Inoue used the expression

$$Z_o \sim U_*^2/g \tag{5}$$

which is based on the work of Kitaigoradski. Equations (3) and (4) imply the assumed logarithmic profile

$$U = U^*/k \log (Z/Z_o) . \tag{6}$$

Now the equation which describes the magnitude of growth rate based on the Miles instability theory and a contribution by Phillips, (1966), can be written

$$B/f = \frac{\rho_a}{\rho_\omega} \frac{2\pi}{C^2 k} \{\frac{A_m \Gamma^2 k^4}{\cos^2 \theta} (- \frac{U''}{U'^3}) Z_m (\int_{Z_m}^{\infty} [U \cos \theta - C]^2 \ell^{-kZ} dZ)^2$$

$$+ A_p \int_o^{\infty} \Gamma^2 (-U'') \cos \theta \, |U \cos \theta - C| \, \ell^{-2kZ} dZ\} \tag{7}$$

where ρ_ω is the density of sea water,

U'' is the mean wind profile curvature,

U' is the mean wind profile slope,

θ is the directional difference between wind and wave,

A_m is a constant and equal to π,

A_p is a constant determined by experiment and Phillips ascertained that the value is $1.6 * 10^{-2}$ with an uncertainty of ±30%,

Γ^2 is +1 above the matched layer and less than +1 below the matched layer.

The first term on the right hand side is Miles' solution and the second term on the right side is Phillips' contribution. It should be noted that B/f is a dimensionless quantity. By substituting the relationships in equations (3), (4), (5) and (6) in equation (7), it can be shown that a relationship exists between B/f and U*/C (dimensionless friction velocity). Several of the above-mentioned investigators have looked at this relationship either on a theoretical basis or in field experiments as seen in Figure 2 (DeLeonibus and Simpson, 1972). Inoue investigated these results and proposed his own curve which is also shown in Figure 2 and can be defined as

$$B(f,U_*) = \{1.39 * 10^{-3}\ell^{-7000}[(U_*/C) - 3.1 * 10^{-2}]^2 + 0.725\,(U_*/C)^2\ell^{-4} * 10^{-4}(C/U_*)^2\}f \qquad (8)$$

If equations (2) and (8) were used in a wave model without any constraints, it is conceivable the waves could continue growing forever. Obviously, this does not occur in nature; therefore, in order to approximate the true situation, the concept of a fully developed sea was introduced. The essence of this concept is that if a wind with the same magnitude blows in the same direction over a given fetch for enough time, the wave spectrum will become fully developed and, no matter how much longer the same wind blows, the spectrum will no longer continue to grow. The Pierson and Moskowitz fully

developed spectrum (1964) was used in the Med model and has the form

$$S_\infty(\omega) = \frac{\alpha g^2}{\omega^5} \omega^{-\beta(\omega_o/\omega)^4} \qquad (9)$$

where $\omega = 2\pi f$

$\alpha = 8.1 * 10^{-3}$

$\beta = 0.74$ and

$\omega_o = g/U_{19.5}$ where $U_{19.5}$ is the wind speed as measured 19.5 meters above sea level.

At each time step, the spectrum at each grid point is compared to the Pierson and Moskowitz spectrum for the given wind. The wave growth routine does not allow the spectrum to exceed the Pierson and Moskowitz spectrum. This is accomplished by modification of equation (1) into:

$$\frac{dS}{dt} = [A\{S/S_\infty)^2\}^{1/2} + BS](1-(S/S_\infty)^2] \ , \qquad (10)$$

whose solution for zero initial conditions is:

$$S(f,t) = A\{\frac{\exp(Bt) - 1}{B}\} [1 + \{\frac{A \exp(Bt) - 1}{BS_\infty}\}^2]^{-1/2} \ . \qquad (11)$$

In order to deal practically with the wave spectrum, it had to be broken into discrete segments. At each grid point the total energy is described by a two-dimensional matrix, 15 frequency bands by 12 direction bands. Thus, for every time step 180 components of the spectrum are investigated at each grid point. Since there are 455 sea points in the Med model,

81,900 pieces of information are calculated at each time step. The compass directions were divided into 30-degree bands because it was assumed that the best existing wind model could not produce wind directions better than ±15 degree accuracy and, of course, the winds are the driving force of any wave model. The frequency bands were limited to 15 to speed the computer calculations and reduce computer memory requirements. For 14 of the frequency bands, the energy is summed over set limits, but for the fifteenth band, the energy is summed from 0.164 cycles/sec to ∞, which, of course, must be truncated for practical reasons. The error caused by truncation is minimal. Table 1 shows the breakdown of the energy spectrum into the frequency and direction bands. The fifteenth frequency is always considered to have a fully developed spectrum since the highest frequencies achieve the fully developed spectrum quite rapidly.

Since equation (11) only provides a one-dimensional spectrum, an equation developed by the Stereo-Wave Observation Project (SWOP) is used to obtain the directional spectra (Inoue, 1967). This equation is

$$F(\omega, \theta, U) = \frac{1}{\pi} [1 + (0.50 + 0.82\, e^{-1/2(\omega U/g)^4} \cos 2\theta + 0.32\, e^{-1/2(\omega U/g)^4} \cos 4\theta] \qquad (12)$$

for $-\pi/2 < \theta < \pi/2$ and θ is the angle between the wind direction and the wave direction and $F(\omega, \theta, U) = 0$, elsewhere.

The directional spectra are computed for 30° increments. As an example, if the wind direction were 180°, the distribution of the wave energy would be as follows: 37.5% of the energy would be placed in the 180° direction band; 25% would be placed in the 150° and 210° bands; and 6.5% of the energy would be placed in the 120° and 240° direction bands. Of course, if the wind direction were 190° rather than 180°, then the energy distribution would be more biased in the 210° and 240° direction bands than in the 120° and 150° bands.

b. Wave Propagation

Waves generated by the same wind system tend to travel as a group. A wave train (a group of waves) travels at a group velocity which is one-half the wave celerity in deep water and exactly the wave celerity in shallow water. Within a group, the various wave frequencies travel at different velocities such that long-period (low-frequency) waves travel faster than short-period (high-frequency) waves. Although waves travel continuously across bodies of water, NYU developed a "jump" technique in the computer model to propagate waves. With this approach, energy as a function of frequency is jumped from grid points to grid points at given time intervals. At every time step, the energy growth is computed for all frequencies at each grid point. When the model has determined that enough time has elapsed for the energy of a given frequency to be transferred to other grid points, then that

energy is transferred all at once instead of gradually as would be the case in a gradient technique. The Med wave model uses a conical conformal grid, true at 40°, with a mesh length of 67 kilometers. The grid system is shown in Figure 3. The time step for this grid system is one hour. With these grid constraints, the higher frequencies are propagated every four hours and the lowest frequencies are propagated every hour. The propagation time for all frequencies is shown in Table 2. Although the spectral energies are computed and propagated in the NYU model on hourly increments, the "jump" technique does not really depict a precise model of the real world and some error is expected in the propagation scheme since energy does not move in such uniform increments in nature.

In the computer model, any given grid point can accept energy from any of its surrounding grid points, depending on the direction from which the waves are propagated. Since the propagation directions are divided into 30° increments, some difficulty arises when energy has to be propagated from a direction other than 0°, 90°, 180° or 270°. The problem is depicted in Figure 4. If the grid point of interest is depicted with an X and the surrounding points are numbered from one to eight, it can be seen that energy can be propagated from points 2, 4, 5 and 7, which correspond to the above directions 315°, 45°, 225° and 135°, respectively. Thus, if the

waves are propagated W from 330°, some of the energy at point X will have to come from grid point 1 and some energy from grid point 2. This is accomplished by propagating from grid points 1 and 2 on alternate time steps. Since new wind fields are read in every six hours, both grid points 1 and 2 would be examined on an equal basis.

c. Wave Dissipation

If the wind is moving against the waves while the waves are propagating, the waves will be dissipated. Inoue developed a formula to account for the wave dissipation if the angle between the wind and wave directions is greater than 75°. The formula is:

$$S_D(f_i,\theta_i) = S_o(f_i,\theta_i)[\ell^{-c\sqrt{S_w}f_i^4}]k(\theta_1) \qquad (13)$$

where $S_D(f_i,\theta_i)$ = spectral component after dissipation,

$S_o(f_i,\theta_i)$ = spectral component before dissipation

f_i,θ_i = center frequency and direction of that component,

c = constant 690 (for ft^2),

$S_w = \Sigma\Sigma S_w(f_i,\theta_i)$

and $k(\theta_1) = 0$ for $\theta \leq 75°$,

$k(\theta_1) = 1.5$ for $\theta \leq 105°$,

$k(\theta_1) = 3.0$ for $105° < \theta_1 \leq 135°$,

$k(\theta_1) = 4.5$ for $135° < \theta_1 \leq 165°$,

$k(\theta_1) = 6.0$ for $165° < \theta_1 \leq 180°$.

3. Mediterranean Winds

A wind model which could be used as a driving force for the Mediterranean wave model had to be developed. The availability of good wind analyses and prognoses is the key to success for any wave model. The two wind models available for use on a routine basis at FNWC are the Tropical Band Grid Analysis with a mesh length 200 kilometers at 35°N and the Marine Wind Analysis and Forecast model with a mesh length of 400 kilometers at 35°N. The Mediterranean basin is a rather complex meteorological area. Its many islands and varying coastline create many localized wind conditions such as "mistrals" off the coast of France and "meltemis" in the Aegean Sea, which cannot be detected in the Tropical Band Analysis or the Marine Wind Field. Ideally, a detailed wind model solely devoted to the Mediterranean Sea is needed. An effort is being made to develop a new Med wind model; however, this is a major undertaking and will not be completed in the immediate future. In order to expedite the wave program, a modified version of the Marine Wind program was developed. The Marine Wind program was chosen even though its mesh length is longer than the Tropical Band grid because it produced both analyzed and forecasted wind fields. The wind field mesh length was reduced by interpolation from 400 kilometers to 67 kilometers. Ship reports were added at analysis time so that local wind conditions missed by the

Marine Wind program would be added to the program. It was recognized that the scheme would not solve all the wind definition problems, but it was hoped that the errors would be kept to a minimum.

It should be noted that all the wave growth formulae developed by NYU which are a function of wind speed or frictional velocity were based on the assumption that the winds were 19.5 meters above the sea surface. The FNWC Marine Wind program also calculates the winds at the 19.5 meter level; however, since it would be rather difficult and tedious to determine individual ships' anemometer heights, the wind velocities from the ship reports were not corrected for anemometer height. Thus, some errors could be expected in the analysis schemes since the wind speed profiles are assumed to be logarithmic over the sea surface and large differences in wind velocities could exist over short vertical distances.

The winds were added to the wave model every six hours. In the North Atlantic wave model, the wind fields were added at an analysis or prognosis time and then used for the next six hours; that is, if the wind input was added at 0Z, then the same winds would be used for every time step up to and including the 05Z time step. It was felt that the wind field would be more representative if the winds were centered about an input time; that is, the 0Z wind fields would be used from

21Z to 02Z and the 06Z fields would be used from 03Z to 08Z. This scheme tended to be superior to the previous techniques except, as will be discussed in Section 4, when strong weather systems entered an area near the end of an analysis or prognosis period. Since the model will use these winds for the entire six-hour period, it will produce large waves sooner than they actually occur.

4. Mediterranean Wind and Wave Verification

The Mediterranean wind/wave model produces analyses and forecasts. Since it is expected for obvious reasons that the analyses probably would be consistently superior to the prognoses, the verification section will be divided into two parts--(a) Wind/Wave Analysis Verification and (b) Wind/Wave Prognosis Verification.

a. Wind/Wave Analysis Verification

Although the optimum method for verifying the wave calculations is to compare the results with data from calibrated wave recorders, there is a scarcity of this type of data in the Mediterranean. Thus, the model verification was accomplished primarily with ship reports. Data from wave recorders will be discussed in a later section.

(1) Shipboard Observations

Under most circumstances visual wave observations, especially by untrained observers, are not the best source of data; however, it was hoped that the density of ship reports would be sufficient enough so that obvious incorrect reports could be eliminated. Ship reports were obtained for a time period extending from May to September 1972. The ship reports were compared only when the analyzed winds were greater than 10 knots. In the original NYU North Atlantic wave spectral model, waves were not grown when the wind speeds were less than 10 knots. This criterion has since been reduced to three

knots so that the energy in the highest frequency band which is not propagated can be properly dissipated. The difference in wave heights generated by a three-knot wind and 10-knot wind is less than 0.2 meters. A total of 451 ship observations was used. The results for wind speed are shown in Figures 5 and 6 and for wind direction in Figures 7 and 8. As seen in Figure 5, 53.7% of the wind speed differences (analyzed-reported) were in the ±2.5 knot category and another 24.8% fell into the ±5 knot category. Less than 6% were in categories greater than ±10 knots. The reported wind speed (negative values) tended to be greater than the analyzed wind speeds (Figure 6), particularly in the ±5 knot range where 38.4% of the comparisons were between -0.1 knots and -5.0 knots. In 19.7% of the cases there were no differences at all.

The wind directions are divided into 30-degree bands (Section 2a). Over 71.8% of the wind direction differences were in the ±15 degree band (Figure 7) and another 12% were in the ±30 degree band. Only 8.6% of the differences were greater than ±45 degrees. Figure 8 indicates that there was little error bias in the wind direction comparisons. It would seem, based on Figures 7 and 8, that the analyzed wind directions are quite good, but the analyzed wind speeds tend to be slightly low.

In addition to shipboard wind observations, observations were also made during airplane flights on

29-30 May 1972 when an airborne wave laser collected data for model verification. These flights will be discussed in greater detail in a later section; however, it is interesting to compare the wind observations with computed winds since the airplane traversed a rather large area in a relatively short time and the wind observations could be considered synoptic. The airplane flew at an altitude of 500 feet. With knowledge of the airplane doppler navigation system, the measured wind velocities can be reduced to ground level. The wind directions should be quite accurate with the measured speeds showing a verification accuracy to within ±5 knots according to Clinton F. Beckner, NAVOCEANO. The airplane winds are shown in Figures 9 and 10. The abscissae of the graphs indicate the time of day. The geographical location of the airplane at the time can be seen in Figure 15. The morning flight on 29 May was made over the Straits of Sicily. The afternoon flight on 29 May and the morning flight on 30 May were made southeast of Sicily. The tail of the arrows indicates the direction from which the wind was coming.

As with the ship reports, the wind directions compared more favorably than the wind speeds. Unlike the ship reports, the wind speed errors do not seem to be biased in either a positive or negative direction.

If the same criteria were used as established for the wind velocity comparisons, then only 223 wave height

observations were available for comparison during the same time period. This is not surprising since ships generally do not report waves as frequently as wind velocity. Wave directions cannot be compared as wind wave and wind directions are assumed to be the same.

The wave height differences (analyzed-reported) are shown in Figures 11 and 12. Nearly 42.9% of the wave height differences were within ±1.5 feet (approximately ±0.5 meters) and 34.1% of the differences were within ±3 feet (±1 meter). Less than 9.9% of the differences were in categories greater than ±4.5 feet. In some of these cases, the large deviations can be explained by either poor wave reporting or poor message transmission as the ships reported wind speeds greater than 20 knots but wave heights of one foot or less. The analyzed wave heights tended to be higher than the reported wave heights. This phenomenon was not expected since the analyzed wind speeds tended to be lower than the reported speeds. Although a definite explanation of this situation is not available as of this writing, several hypotheses exist. There is a possibility that the wave energy in the computer model grows at a faster rate than it does in the physical world. The growth equations were originally developed for the North Atlantic Ocean where the fetch and duration of a given wind are probably longer than they would be in the Mediterranean Sea. It is possible that the growth equations will have to

be refined for the Mediterranean Sea; however, it is interesting to note that the only available set of field data where wave heights increased from a calm sea to approximately 3.0 meters indicated that the growth rate was on the order of 0.6 meters per hour for a 14 m/sec wind speed. The computer model had the same growth rate. Thus, the above argument will have to be held in abeyance until additional data become available which can either confirm or refute the argument. This data set will be discussed in more detail in later paragraphs.

Another explanation may be that the ship observers underestimate the wave heights. A check was made of the correlation between reported wind speeds and the associated wave heights. It appeared that the wave heights were much lower than would be expected for a given wind speed, no matter what the fetch might be. Generally speaking, this problem does not seem to be too serious since 77% of the wave height differences fell between ±3 feet (±1 meter).

Several decisions had to be made before swell heights and directions could be compared. First, there has been considerable speculation as to whether shipboard observers are able to differentiate between wind waves and swell. A check was made of the Mediterranean shipboard observations to determine if observers were differentinating between wind waves and swell. It was determined that in 64% of the ship reports evaluated, the swell and wind (wave

direction assumed to be the same as wind) were within ±60 degrees of each other. If the climatological and geographical make-up of the Mediterranean basins is considered, this ratio probably is not out of proportion; however, it was decided to evaluate the reported swell directions very carefully before comparing the data to the model results.

Another point to consider is the method by which the Mediterranean wave model computes wave heights and directions. As mentioned in Section 2a, the model computes and propagates wave energy rather than wave heights. At any given grid point, the wave energy is the sum total of all the energy in the 12 direction bands by 15 frequency bands matrix. It would be impractical in terms of computer output time and the volume of output generated to display the spectra at every grid point. Instead, the spectra are displayed at representative grid points and significant wave heights, $\tilde{H}_{1/3}$ (by definition the average height of the highest one-third waves) is displayed for all grid points. The significant wave height by definition is

$$\tilde{H}_{1/3} = 4\sqrt{E_{TOTAL}} \tag{14}$$

where E_{TOTAL} is the total wave energy at a grid point. The wave direction is determined by investigating the total energy in each direction band and then selecting the band which contains the modal energy. If the modal wave direction at a grid

point is not the same as the wind direction, then the wave is assumed to be swell rather than a wind wave. One problem that arises with this approach is that if a secondary wave front exists, it could be difficult to ascertain from a printout of wave heights and directions. The spectra output for the selected grid points, which hopefully represent the entire Mediterranean Sea, would have to be carefully analyzed.

Because of the above limitations, it was decided to use only ship data from 10-15 April, 24-28 April and 25-30 May 1972 for swell comparisons. These dates were selected because hindcast studies had been made with the wave spectral model for comparison with data from a SACLANT (Supreme Allied Command-Atlantic) ASW Research Centre wave buoy and NAVOCEANO airborne wave laser. The analyses and ship reports for these time periods were reviewed very carefully. Comparisons were only made when it was felt that the ships were actually reporting swell and not wind waves. Even with careful quality control, there were still ship reports which were used for comparison that might have been eliminated.

The comparisons between analyzed and reported swell heights and directions are plotted in Figures 13 and 14, respectively. Since approximately 30% of the ship reports contained swell observations and many of these reports were not available because of the above restraints, only 61 ship reports

were available for comparison. Over 90% of the differences (analyzed-reported) were within ±3 feet (±1 m), with 70.5% within ±1.5 feet (±0.5 m). The swell directions compared almost as well as the swell heights. About 72.1% of the differences were within ±30 degrees and another 14.7% within ±60 degrees. Neither the swell height or direction differences seemed to be biased in either a positive or negative direction.

Some of the direction differences could be readily explained. In one case where the error was +180 degrees, it was quite apparent that the computer model took approximately three hours longer than it should have to propagate swell which was coming from due west to the ship position (33.9°N, 28.3°E). Since there was only one ship report from all three studies available in the far eastern Mediterranean Sea, it is difficult to determine if the model has an inherent propagation problem in the eastern Mediterranean Sea, where the swell can move in a longer continuous path than in any other area in the Mediterranea, or if this was an isolated problem. This situation does not seem to occur in the western or central Mediterranean basins; however, in these areas, swell can only propagate over relatively short distances before encountering land. In at least two other cases where the differences were equal to or greater than ±90 degrees, computed swell probably did exist at the ship position but the printout of wave spectra from the closest grid points seemed to indicate that the computed

wind waves dominated the computed swell rather than vice versa as indicated by the ship reports. Clearly this type of problem can only be resolved with wave data measured by accurate recorders. Some of the differences (of between ±30 and 60 degrees) can be attributed to the method by which the computer model propagates waves. As discussed in Section 2b, the computer model does not propagate wave energy from all compass directions at every time step; instead it propagates from alternate directions. Thus, at any given time step, the computed wave direction could vary by as much as 30 degrees from the previous time step. If one considers all the assumptions that had to be made in invesgigating the swell parameters and that the Mediterranean Sea contains many little islands which could easily obstruct swell propagation, then it does appear that the model handles swell propagation satisfactorily. Waves will again be analyzed in the next section in terms of frequency or period. Since measured wave data will be reviewed, fewer assumptions will have to be made than were made with shipboard observations.

(2) Measured Wave Data

The only measured wave data available for this study were obtained from a Datawell Waverider Buoy System operated by the SACLANT ASW Research Centre and an airborne wave laser operated by NAVOCEANO. Measurements from the Waverider were made on 10-15 April and 25-29 May 1972. On the first occasion the buoy was located at 43°30'N, 08°30'E

(Ligurian Sea). These data were only compared to the computer wave analysis. On the second occasion the buoy was located at 37°23'N, 11°36'E (Straits of Sicily). These data were compared to both computer analyses and 24-hour prognoses. The buoy locations are shown in Figure 15. The Datawell Waverider actually measures vertical acceleration and must be doubly integrated to obtain wave heights. The Datawell Waverider Buoy System has proved to be a highly reliable and accurate instrument for measuring waves. The wave spectra computed from the Waverider were supplied by Dr. Melbourne Briscoe, SACLANT oceanographer.

The computed and measured wave spectra cannot be compared exactly since the wave spectra from the buoy data are computed for individual frequencies while the wave energies in the computer model are computed for frequency bandwidths. The distribution of the bandwidths is shown in Table 2. First, it should be noted that the bandwidths are not equal in size. This tends to produce some unevenness in the wave spectra. The high frequency band theoretically includes all the gravity wave energy from 0.164 to ∞ cycles/sec. Thus, the first point in the computed wave spectra usually appears as a spike. To compare the computed and measured wave spectra exactly, the wave energy for the individual frequencies in the measured spectra would have to be summed and then compared to the energy in a given frequency band of the computed spectra.

Since this would be a rather arduous task, two other parameters that can be more easily deduced from the spectra will be compared. These parameters are the dominant frequencies and $\bar{H}_{1/3}$.

The measured wave spectra from 13-14 April were compared to computed data from grid points 15 (43.89°N, 7.96°E) and 26 (43.23°N, 8.01°E) and are shown in Figures 16-21. Since there was an interval of calm seas during 25-29 May, only selected wave spectra are shown in Figures 24-29. These spectra demonstrate the growth of waves from calm to turbulent conditions. During this time period, computed spectra from grid points 220 (37.32°N, 11.82°E), 221 (37.33°N, 12.66°E), 250 (36.55°N, 11.83°E) and 251 (36.66°N, 12.67°E) were used for comparison. The laser wave spectra comparisons are shown in Figures 30-31. Generally speaking, the computed spectra compared rather well to the measured spectra. Some variation did occur in several of the comparisons and these anomalies will now be described.

First, the significant wave height differences for the 13 April wave spectra (Figures 16-19) were less than 0.1 meters. On 14 April (Figures 20-21) the differences increased to approximately 0.5 meters. The source of error probably can be attributed to the 14 April, 12Z computer wind analysis in the vicinity of the wave buoy implantment. The wind analysis was strongly influenced by three ship reports that contained wind speeds of 25 knots and were 120 to 170 nautical miles

(three or four grid mesh lengths) west of the buoy. The true wind speeds at the buoy site probably were less than the calculated wind speeds; however, the SACLANT ASW Research Centre did not provide wind data for this time period and there were no other ships in the immediate area to provide the actual wind speeds in the area of interest. It is interesting to note that the second wave spectrum based on 14 April buoy data did increase slightly in magnitude, but since the time sequence did not extend any further, it could not be determined if the measured $\tilde{H}_{1/3}$ would eventually approach the computed $\tilde{H}_{1/3}$. A similar situation occurred on 28 May when the computed $\tilde{H}_{1/3}$ at 12Z was almost twice as large as the measured $\tilde{H}_{1/3}$ (Figures 25-26) and two hours later the difference in magnitude of the significant wave heights was approximately 0.1 meter. This situation is definitely a function of the method used by the model to input winds (Section 3). This set of data will be discussed further in the next several paragraphs.

On 13 and 14 April, the dominant frequencies of the measured data were on the order of 0.2 Hz. The dominant frequency band of the computed spectra was the highest band (0.164 Hz to ∞). Thus, there is a high degree of correlation between the computed and measured dominant frequencies.

Dr. Briscoe states that the nature of waves in the western Mediterranean Sea is such that the predominant frequency usually lies between 0.2 Hz and 0.3 Hz. The computer

model does not presently have this degree of resolution, but the computed high frequency band could be shifted to account for the higher frequencies at the expense of the lower frequency bands which apparently have little significance in the Mediterranean Sea. An unpublished climatology study (Lazanoff, 1972) indicates that the percentage of wave frequencies less than 0.05 Hz was on the order of 2% or less.

The first two computed spectra on 13 April had a second energy peak in the vicinity of 0.1 Hz. The measured data did not have this peak. Since the secondary energy peak significantly diminished by 18Z, 13 April, this may be an indication that the wave model is not dissipating energy as fast as it should. Again, since there was only one set of data where this situation occurred, it is difficult to make a general statement about the dissipation techniques of the computer model.

For the most part, the wave spectra comparisons for 25-29 May seem to be better than the April comparisons. Wind speeds and $\bar{H}_{1/3}$ are plotted for the entire time period in Figures 22 and 23. As mentioned previously, the computed $\bar{H}_{1/3}$ was almost twice as large as the measured $\bar{H}_{1/3}$ at 12Z, 28 May (Figure 25) and two hours later, the difference in significant wave heights was on the order of 0.1 meter (Figure 26). The rather large error at 12Z can be attributed to the wind cycling method used by the model to input wind

velocities. This can be demonstrated by examining the graphs in Figure 23. The computed and measured wave heights and wind speeds from 20Z, 27 May to 12Z, 29 May are plotted. Wind directions were not shown since the directions never varied from the 300° to 330° range during the entire time period. Although the plots indicate there is good agreement between the wind analyses and measured wind speeds, it must be remembered that the wind analyses are only produced every six hours and cannot reflect any fast-moving changes such as occurred between 04-06Z, 28 May. Thus, if the winds have high velocities for a short duration near analysis time, the model could over-grow waves since the same wind analysis is used for six hours (Section 3). This is precisely what occurred at 12Z, 28 May. Although the wind velocities did not become large until 11Z, the wind analysis reflected these winds at 09Z, permitting the model to grow the large waves two hours sooner than they actually occurred. The inverse could also occur, i.e., the analyzed winds could be too low for several hours and the wave growth would lag by the same amount of time. The obvious solution to this problem would be to increase the number of input wind fields per time steps. FNWC is investigating a more sophisticated wind analysis for the Mediterranean. The wind fields will be produced on a fine mesh length and be based on both land and sea reports. If the product is better than the present wind analysis, then the wind analysis techniques used in the wave spectral model will be modified.

As of now the analysis time can be considered accurate within ±3 hours.

The wave heights shown in Figure 23 indicate that, given the correct wind speed, the model appears to be growing waves at the proper rate. This subject has already been discussed in the paragraphs describing the analysis of observed wave heights from ships.

The airborne wave laser was installed aboard a NAVOCEANO P-3A airplane. Flights were made on 29-30 May 1972. The wave measuring instrument is a standard Geodolite 3-A airborne altimeter, which is a continuous wave helium-neon laser, manufactured by Spectra Physics, Inc. The helium-neon laser is described in detail by Ross, Peloquin and Sheil (1968) and Ross, Cardone and Conaway (1970). The airplane tracks were flown in pairs--upwind and downwind--at an altitude of 500 feet. This approach is used so that the speed of the aircraft relative to the phase speed of each wave frequency component can be accounted for without too much difficulty when the moving coordinate system of the aircraft is converted to fixed coordinates. Since, in this case, it is assumed that all waves are traveling in the direction of the wind, the presence of swell from other directions and the spreading of wave energy with distance can lead to errors [Schule, Simpson and DeLeonibus (1971)]. During 25-29 May the range of wind directions remained within 280°-320° so that the swell was moving in the same

direction as the wind waves and this type of error should be at a minimum. Errors due to wave dispersion should also be at a minimum since airplane tracks for 29 May, as shown in Figure 15, were made in narrow areas. Unfortunately, due to instrument failure, the laser data on 30 May were inaccurate and will not be discussed in this paper.

Airplane motion can distort the laser data. The full effect of the motion is not fully understood. Ross et al. (1970) indicated that the disturbances would probably occur in the low frequency range (.065 Hz or less). Since a wave climatology study (Lazanoff, unpublished report) has indicated that the swell frequencies seldom reach or exceed this range, errors due to airplane motion should also be at a minimum.

Usually waves are measured by a stationary wave recorder and wave spectra are computed from a finite length of data. Since the airplane is not stationary, the computation of wave spectra from the laser is complicated. The airplane flew at speeds that ranged from 235 to 265 knots. Thus, the laser wave spectra is a function of distance as well as time. If a small enough time interval can be selected and the airplane flies over deep water, then it can be assumed that the wave spectrum is representative of one location. In this case, the laser recorded data every second for 30 minutes on each track. The spectra were computed for three-minute intervals (approximately 12.5 miles).

Comparisons of spectra from the wave laser with the computed spectra are shown in Figures 30 and 31. Spectrum from the wave buoy is also shown in Figure 30. The wave buoy spectrum agrees with the laser spectrum. The significant wave heights and the predominant frequencies (approximately 0.13 Hz) compared extremely well. Both measured spectra show a secondary frequency peak at 0.1 Hz which does not appear in the computed spectrum. The secondary energy peak is a definite indication of swell. Since the model does not have this peak. this may be an error similar to the problem noted in the swell analysis section where it seemed that the swell did not propagate energy fast enough in the eastern Mediterranean.

The comparison between ship reports, measured data and computer calculations seems to indicate that the wind and wave analyses have a high degree of accuracy. The wave analyses, as well as the 24-hour prognoses, are being transmitted to Rota, Spain, twice a day (0Z and 12Z) on an operational basis.

b. Wind/Wave Prognosis Verification

Since it has been shown in the previous section that, given the correct wind velocity, the computer model will produce accurate wave spectra, the principal concern of this section is to determine if the wind prognoses are valid. To reiterate what has already been mentioned in Section 3:

the Med wind prognoses are interpolated from the FNWC Marine Wind fields. The grid of the Marine Wind model has a mesh length on the order of 400 kilometers at 35°N. The Mediterranean grid has a mesh of 67 kilometers; thus, most local wind conditions will not be predicted with this scheme. Unlike the Med wind analyses, the prognoses cannot be modified with ship reports. Wind prognoses are made every six hours out to 48 hours. It can be assumed that the more time that has elapsed from the analysis time, the less accurate the prognosis. Since FNWC decided to transmit the 24 prognoses to FWC, Rota, only these prognoses are discussed in this section.

Wind prognoses from three grid points--175 (37.5°N, 4.5°E), 220 (37.5°N, 12°E), and 372 (35°N, 28°E)--were selected for verification. The grid points were to represent the Eastern and Western Mediterranean Basins and the Straits of Sicily. The prognoses for grid points 175 and 220 were compared to ship reports when available (there were no ship reports available in the vicinity of point 372 during the verification period). Prognoses for grid point 220 were also compared to measured winds in the vicinity of the SACLANT wave buoy for the period 25-29 May. For the remainder of the verification period (30 May-6 June), the prognoses were compared to the computer analyses and the FWC, Rota 24-hour prognoses (26 May-1 June). The same comparisons were made during 28 May-6 June for grid points 175 and 372. In addition, 24-hour prognoses were compared to wind velocities measured by

the NAVOCEANO airplane on 12Z, 29 May and 12Z, 30 May. The above comparisons are shown in Figures 32-36. The plotted wind directions are the directions toward which the winds are moving.

Although there were not many cases of high wind speeds, one significant observation can be made from the plots. The prognoses, unlike the analyses, tend to lag behind the actual movement of weather systems by approximately 12 hours. This was not totally unexpected. The Marine winds are computed from surface pressure fields generated by the FNWC Primitive Equation (PE) multi-layer model. It has been shown that the PE model has a tendency to move weather systems too slowly over the North Pacific by 15% and over the North American continent by 25% (Osburn, 1971). It would seem reasonable that this tendency would extend to the Mediterranean Sea.

The computer prognoses were compared to the FWC, Rota hand prognoses to determine if one method was consistently superior to the other. The computer prognoses appeared to be superior at grid points 220 and 372. For example, as seen in Figure 1, the hand prognosis completely missed the weather system which passed over grid point 220 at approximately 12Z, 28 May. The computer prognosis did predict the system, although 12 hours too late. The hand prognosis seemed to do better at grid point 175. The superiority may be due to the geographical proximity of FWC, Rota to the grid point. Several U.S. Navy air squadrons are stationed

at Rota and the weather central may be able to obtain meteorological information from these squadrons which is not available to anyone else. Although there wasn't much difference, the computer prognoses did seem to compare better to the airplane winds as seen in Figure 36 than the hand prognoses.

Another interesting point about the computer prognoses that was not revealed in the above study is that in the northwest Mediterranean (in the vicinity of France), a consistent error seems to occur. The model tends to over-compute wind speeds in this area. This may be due to the close proximity of the French Alps to the Mediterranean. Although pressure fields over mountains are supposed to be corrected to sea level pressure, the predicted pressure gradients seemed to be rather tight. This may be due to the coarseness of the original grid or the inaccuracy of the sea level pressure reduction.

Although the Med wave spectral model has been operational since April 1972, significant storms did not occur in the Mediterranean until late October 1972. Twenty-four-hour forecasts and analyses of wave heights are shown in Figure 37 for 31 October-2 November. Ship reports are indicated on the analysis plots. The analyses, prognoses and ship reports show good agreement. During this time period, a storm passed over the Aegean Sea. Maximum significant wave heights were on the order of 15 feet. The analyzed and

forecasted wind velocities are plotted in Figure 38 for a selected grid point, 194, in the Aegean Sea. The forecasts and the analyses compared quite satisfactorily with each other as well as with ship reports. As of 12Z, 31 October, the prognoses appeared to lag behind the analysis by 12 hours. The lag can be seen more easily in the wind direction plots than in the wind speed plots. The movement of the wave system shown in Figure 37 seems to confirm the prognosis lag. It may be that the rate of movement of forecasted weather systems in the Mediterranean will have to be adjusted by artificial means.

5. Conclusions

The Mediterranean wave spectral computer model is the first spectral model to be used operationally for analyses and prognoses. The model has two basic parts--wind computation and wave energy computation. The wind analyses were compared to ship reports and, for a two-day period, winds were measured from an airplane. Although the analyzed wind speeds and wind directions compared rather well with the observed data, the wind directions appeared to be more accurate than the wind speeds which tended to be too low. For the most part, the analysis scheme seemed to propagate weather systems at the proper rate of speed; however, some error did seem to occur because the wind field inputs to the wave model were only changed every six hours (one hour per time step). Although further investigation is needed on this subject, it would seem that if the wind inputs were increased to one every three time steps, significant improvement in the wind analysis would occur. FNWC is currently investigating a new wind analysis scheme for the Mediterranean Sea. If the new scheme proves to be a significant improvement over the current operational wind analysis, then it will be inserted into the Mediterranean model.

The wind prognoses were not compared to measured data as extensively as the wind analysis; however, it was apparent from observation of the 24-hour prognoses that the prognoses generally lagged behind the analysis by 12 hours. This

error could be attributed to the surface pressure fields computed by the FNWC PE boundary layer model which are the initial input to the prognosis scheme. The wind prognoses could also be improved by developing a finer mesh length for the initial wind calculations.

The computed wave spectra and significant wave heights were compared to ship reports, wave spectra obtained from a SACLANT Wave Buoy and a NAVOCEANO airborne wave laser. The basic conclusion is that, given the correct wind velocity, the computer model computes the proper spectra. It is interesting to note that the wave energy growth equations which were originally developed for the North Atlantic Ocean seemed to be accurate in the Mediterranean Sea. Two points could be investigated in greater detail. First, the frequency bandwidths of the computed wave spectra could be modified so that the highest frequency band is subdivided into smaller bandwidths. This would not affect the basic calculations of wave energy, but would permit closer observation of the energy levels in the higher frequency ranges. This could be of use to underwater acousticians who are interested in high-frequency ambient noise problems. Finally, a limited amount of data seemed to indicate that the model was propagating swell (or energy in the lower frequencies) too slowly. A field test should be conducted to determine if the swells are being propagated at the proper rate.

References

Baer, L., An experiment in numerical forecasting of deep water ocean waves. Lockheed Missile and Space Co., Sunnyvale, Calif., 1962.

Barnett, T. P. and J. C. Wilkerson, On the generation of wind waves as inferred from airborne measurements of fetch-limited spectra, Journal of Marine Research, 25(3), 1967.

Cardone, V. J., Specification of the wind distribution in the marine boundary layer for wave forecasting, Dept. of Meteorology and Oceanography, New York University, TR 69-1, 131 pp., 1969.

DeLeonibus, P. S. and L. S. Simpson, A case study of duration-limited wave spectra observed at an open ocean tower, Journal of Geophysical Research, 77(24) pp. 4555-4569, 1972.

Inoue, T., On the growth of the spectrum of a wind generated sea according to a modified Miles-Phillips mechanism and its application to wave forecasting, Dept. of Meteorology and Oceanography, New York University, TR 67-5, 74 pp., 1967.

Lamb, H., Hydrodynamics, 6th edition, Cambridge University Press, 1932.

Lazanoff, S., Summary of wind and wave climatology for the Mediterranean Sea, NAVOCEANO unpublished memo, 1972.

Miles, J. W., On the generation of surface waves by shear flows, Journal of Fluid Mechanics, 3(2), pp. 185-204, 1957.

Osburn, J. C., An evaluation of 36-hour forecasts of small-scale disturbances (SD) at 500 MBS for November 1971, FNWC unpublished report, 1972.

Phillips, O. M., The Dynamics of the Upper Ocean, Cambridge University Press, 261 pp., 1966.

Pierson, W. J. and L. I. Moskowitz, A proposed spectral form for fully developed wind seas based on the similarity theory of S. A. Kitaigorodskii, Journal of Geophysical Research, 69(24) pp. 5181-5190, 1964.

Ross, D. B., R. A. Peloquin and R. J. Sheil, Observing ocean surface waves with a helium-neon laser, Fifth Symposium on Military Oceanography, Panama City, Florida, 18 pp, 1968.

Ross, D. B., V. J. Cardone and J. W. Conaway, Jr., Laser and microwave observations of sea-surface condition for fetch-limited 17-to-25 m/s winds, IEEE Transactions on Geoscience Electronics, VIGE-8, Number 4, pp. 326-336, 1970.

Schule, J. J., L. S. Simpson and P. S. DeLeonibus, A study of fetch-limited wave spectra with an airborne laser, Journal of Geophysical Research, 76(18), pp. 4160-4171, 1971.

Snyder, R. L. and C. S. Cox, A field study of the wind generation of ocean waves, Journal of Marine Research, 24(2), pp. 141-177, 1966.

Central Frequency (H_z)	Central Period (Seconds)	Frequency Bandwidth (H_z)
0.164	6.1	.164 - ∞
0.153	6.5	.142 - .164
0.133	7.5	.125 - .142
0.117	8.6	.108 - .125
0.103	9.7	.097 - .108
0.092	10.9	.086 - .097
0.083	12.0	.080 - .086
0.078	12.9	.075 - .080
0.072	13.8	.069 - .075
0.067	15.0	.064 - .069
0.061	16.4	.058 - .064
0.056	18.0	.053 - .058
0.050	20.0	.047 - .053
0.044	22.5	.042 - .047
0.039	25.7	.036 - .042

Energy in these frequency bands is ordered in twelve (12) 30 degree direction bands starting with the cardinal direction north

TABLE 1

MEDITERRANEAN SPECTRAL FREQUENCIES VS DISTANCE TRAVELED / HR. AND TOTAL TIME FROM GRID POINT TO GRID POINT

FREQUENCY (HZ)	DISTANCE (NM) TRAVELED /HOUR	ELAPSED TIME (HR) FROM GRID POINT TO GRID POINT
0.15278	9.75	4
0.13333	11.25	3
0.11667	12.90	3
0.10278	14.55	2
0.09167	16.35	2
0.08333	18.00	2
0.07778	19.35	2
0.072222	20.7	1
0.06667	22.5	1
0.06111	24.6	1
0.05556	27.0	1
0.05000	30.0	1
0.04444	33.75	1
0.03889	38.55	1

TABLE 2

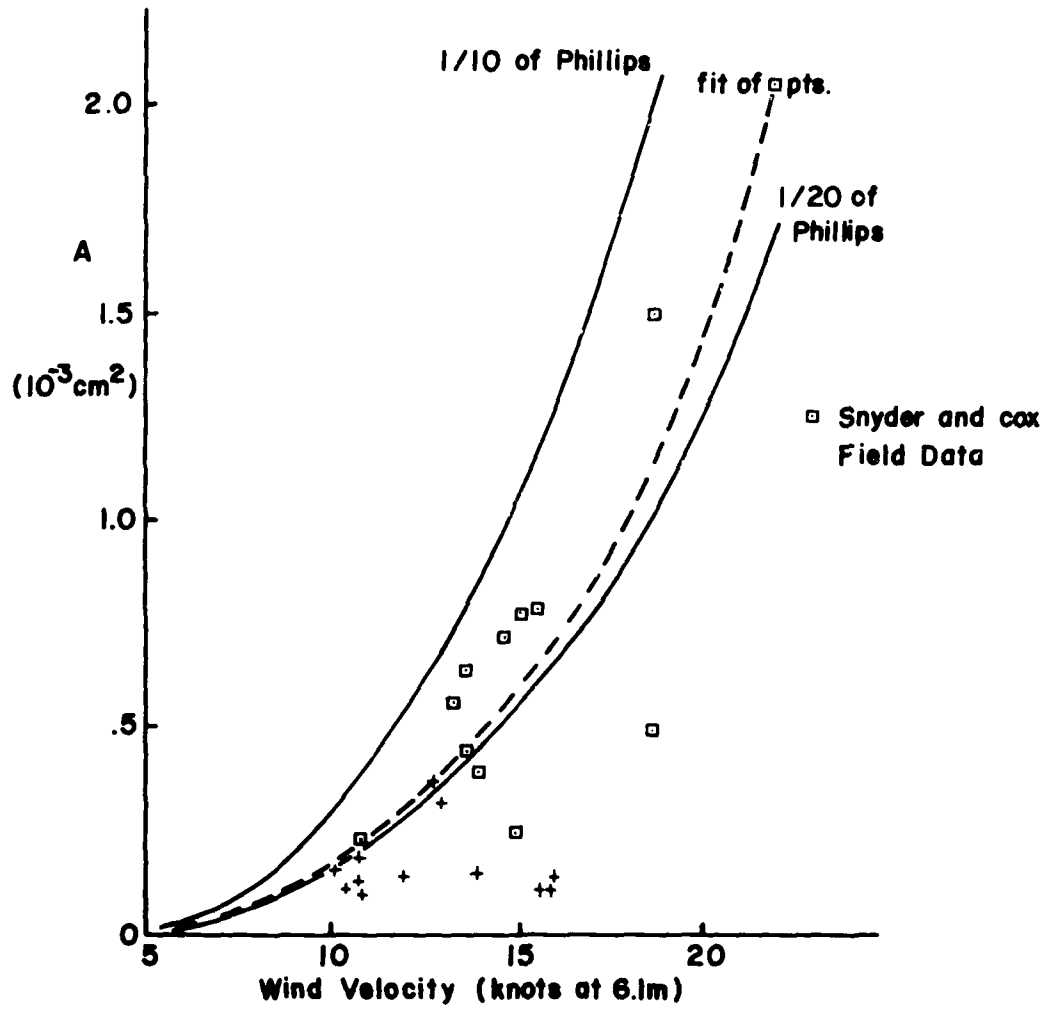
1/10 of Phillips
fit of pts.
1/20 of Phillips
Snyder and cox Field Data
A
$(10^{-3}cm^2)$
2.0
1.5
1.0
.5
0
5
10
15
20
Wind Velocity (knots at 6.1m)

FIGURE 1

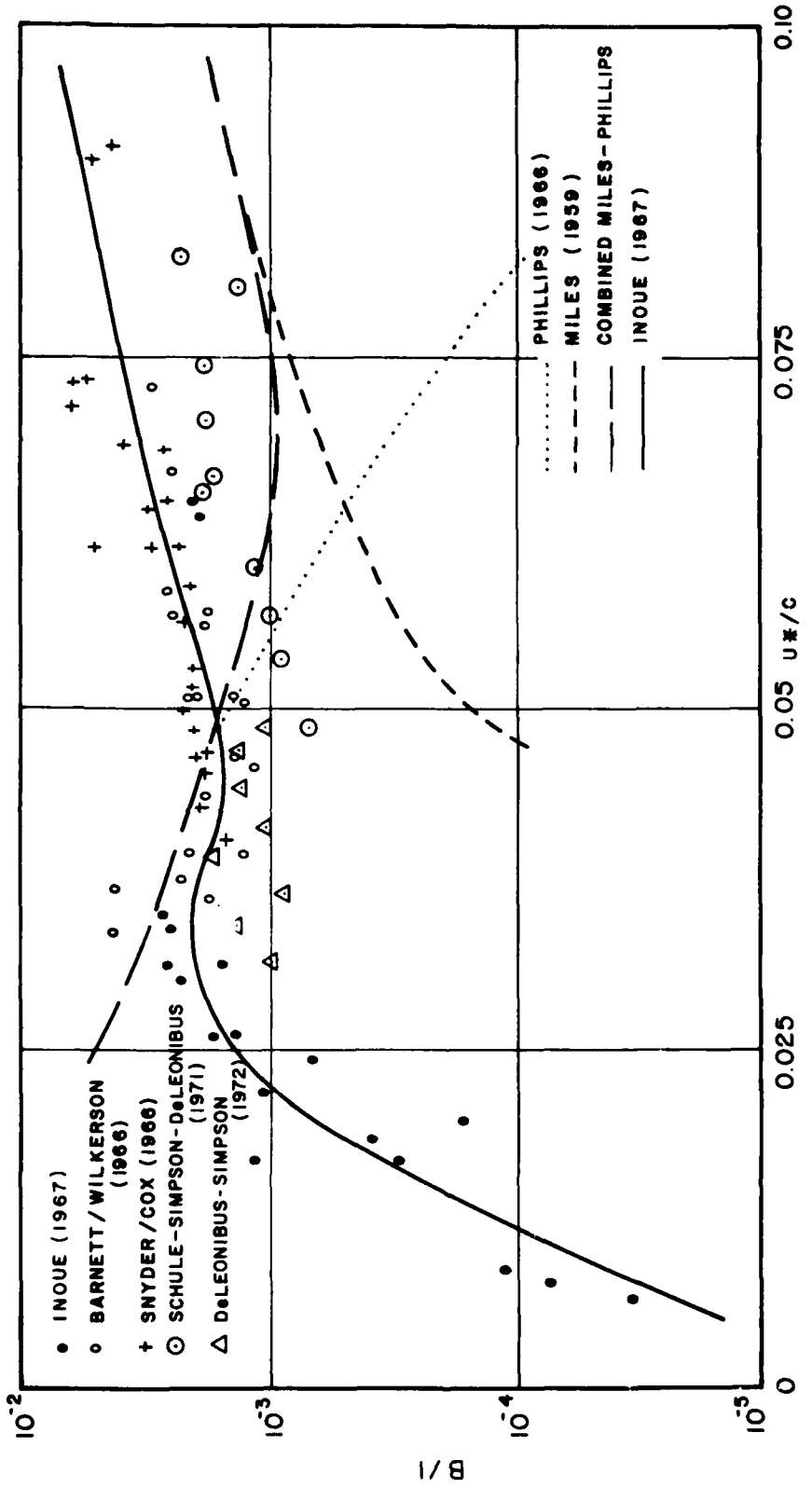
B/I
10^{-2}
10^{-3}
10^{-4}
10^{-5}
0
0.025
0.05 u*/c
0.075
0.10
• INOUE (1967)
o BARNETT/WILKERSON (1966)
+ SNYDER/COX (1966)
⊙ SCHULE-SIMPSON-DeLEONIBUS (1971)
△ DeLEONIBUS-SIMPSON (1972)
PHILLIPS (1966)
MILES (1959)
COMBINED MILES-PHILLIPS
INOUE (1967)

FIGURE 2

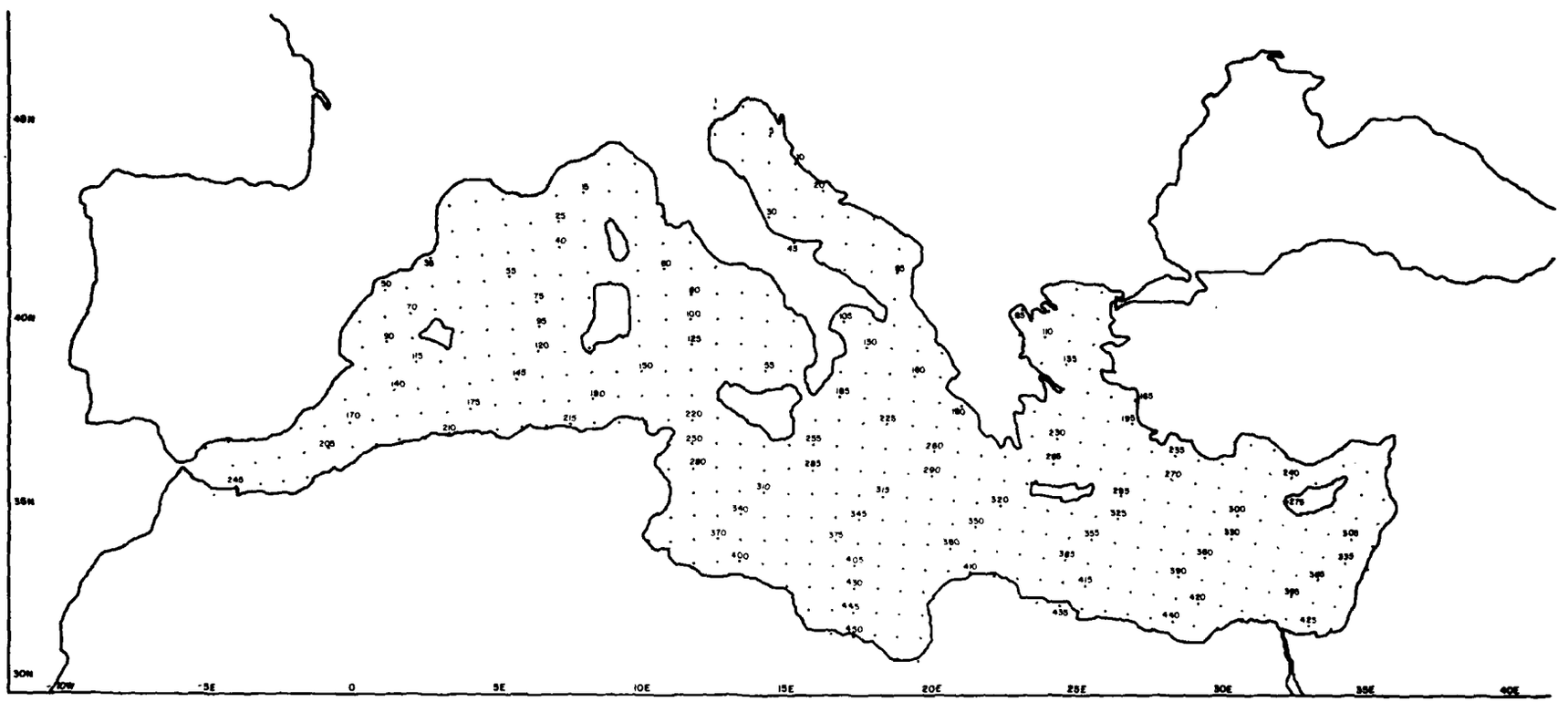

MEDITERRANEAN SEA GRID SYSTEM

FIGURE 3

PROPAGATION OF ENERGY FROM GRID POINT TO GRID POINT

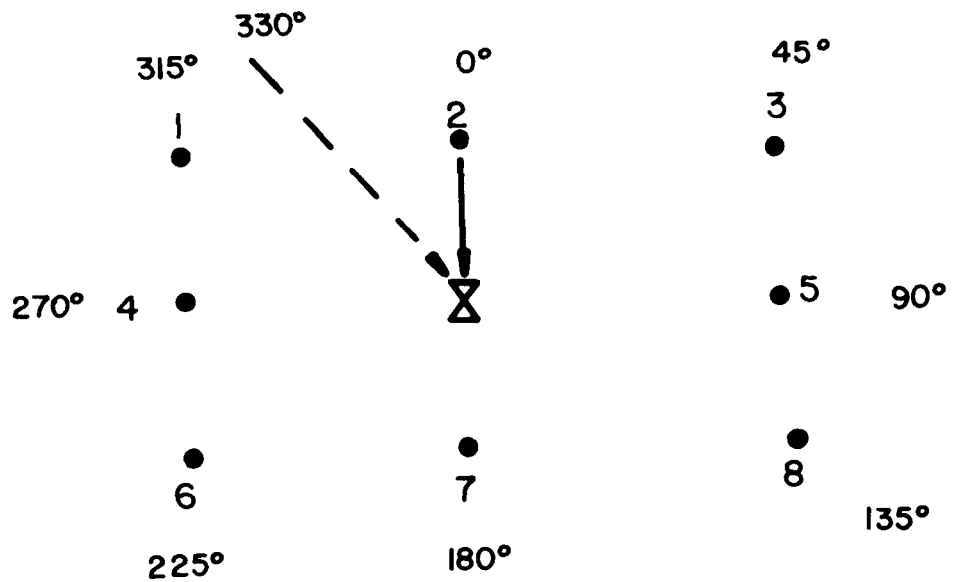

ENERGY PROPAGATED DIRECTLY FROM GRID POINT TO GRID POINT

ENERGY PROPAGATED FROM ADJACENT GRID POINTS ON ALTERNATE TIME STEPS

FIGURE 4

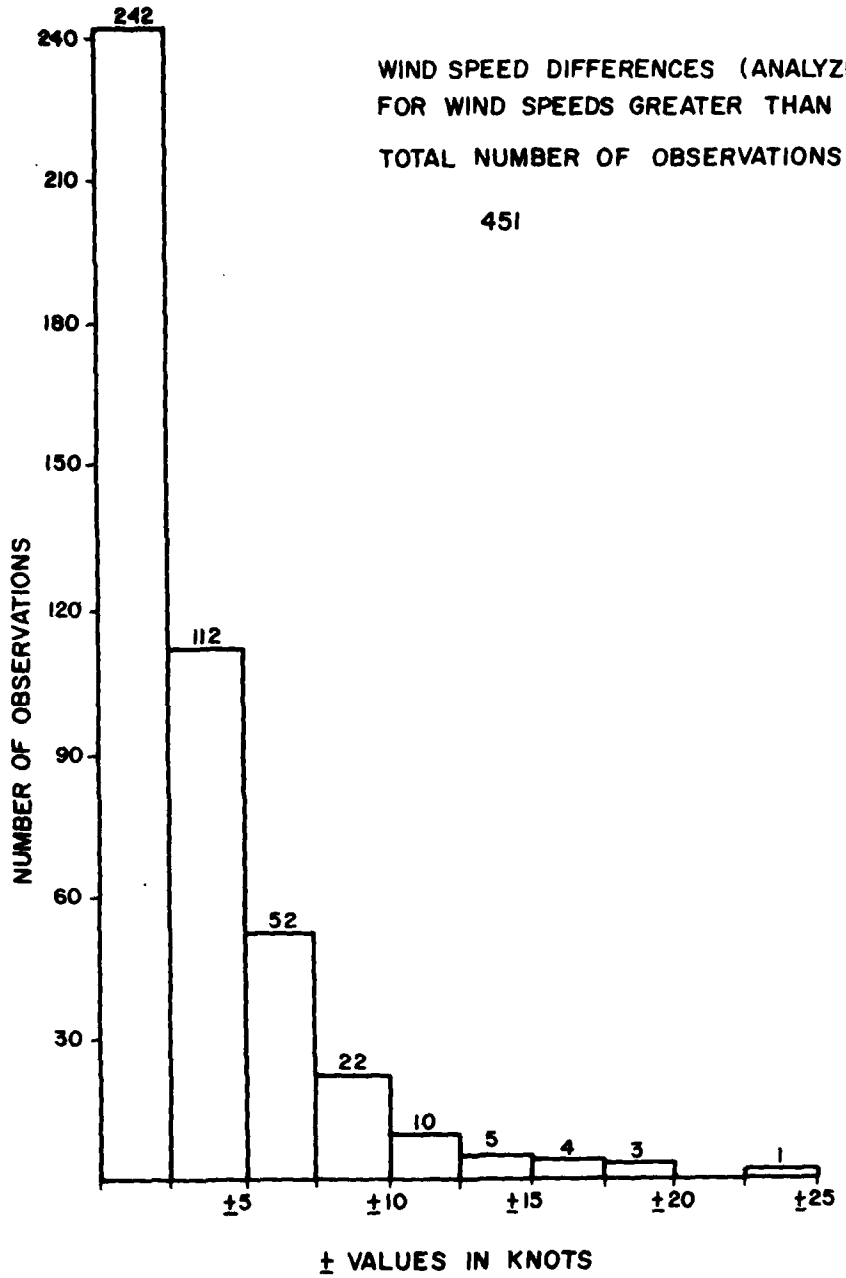
WIND SPEED DIFFERENCES (ANALYZED-REPORTED)
FOR WIND SPEEDS GREATER THAN 10 KNOTS
TOTAL NUMBER OF OBSERVATIONS
451
NUMBER OF OBSERVATIONS
240
210
180
150
120
90
60
30
242
112
52
22
10
5
4
3
1
±5
±10
±15
±20
±25
± VALUES IN KNOTS

FIGURE 5

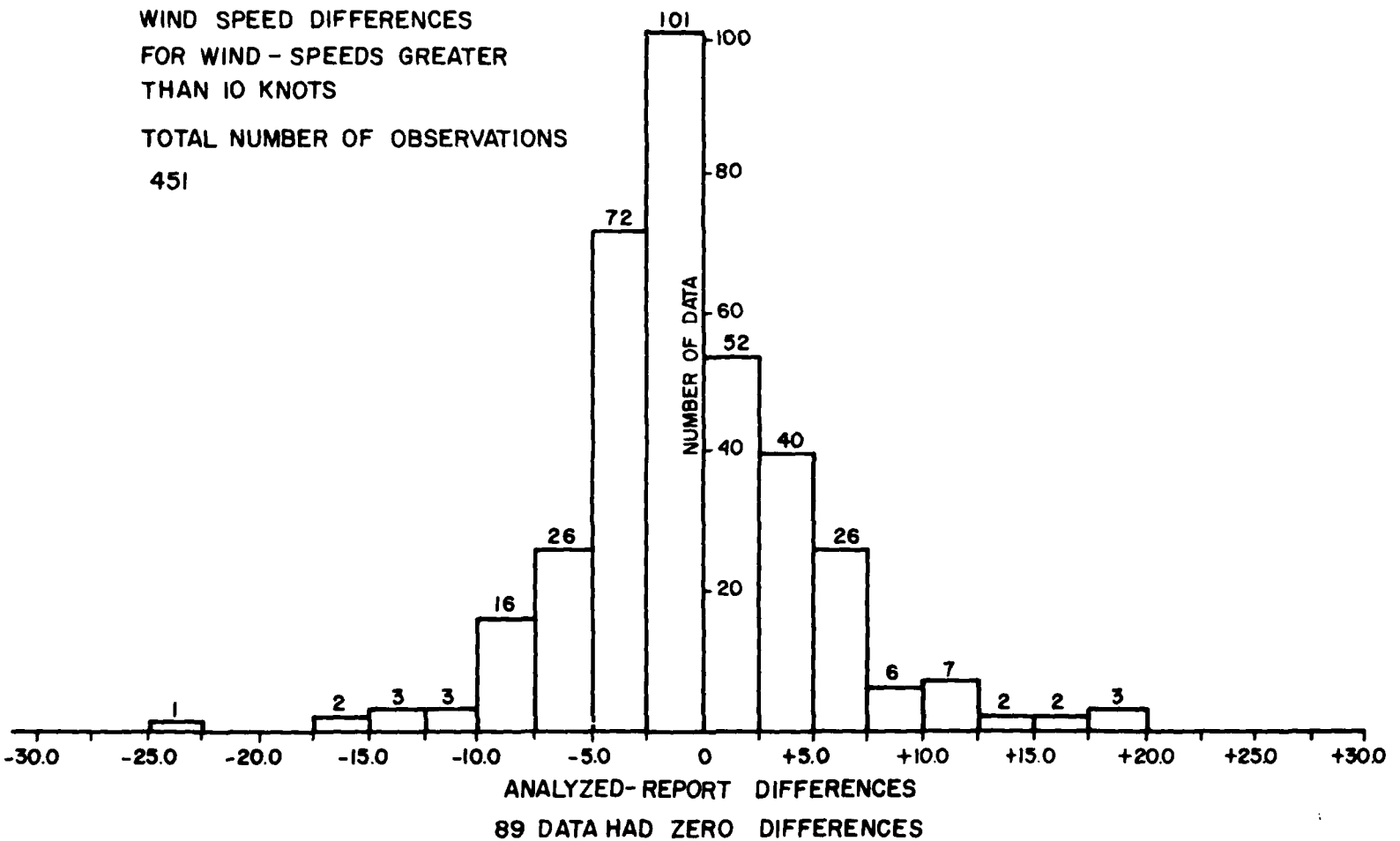
WIND SPEED DIFFERENCES
FOR WIND - SPEEDS GREATER
THAN 10 KNOTS
TOTAL NUMBER OF OBSERVATIONS
451
NUMBER OF DATA
100
80
60
40
20
1
2
3
3
16
26
72
101
52
40
26
6
7
2
2
3
-30.0
-25.0
-20.0
-15.0
-10.0
-5.0
0
+5.0
+10.0
+15.0
+20.0
+25.0
+30.0
ANALYZED- REPORT DIFFERENCES
89 DATA HAD ZERO DIFFERENCES

FIGURE 6

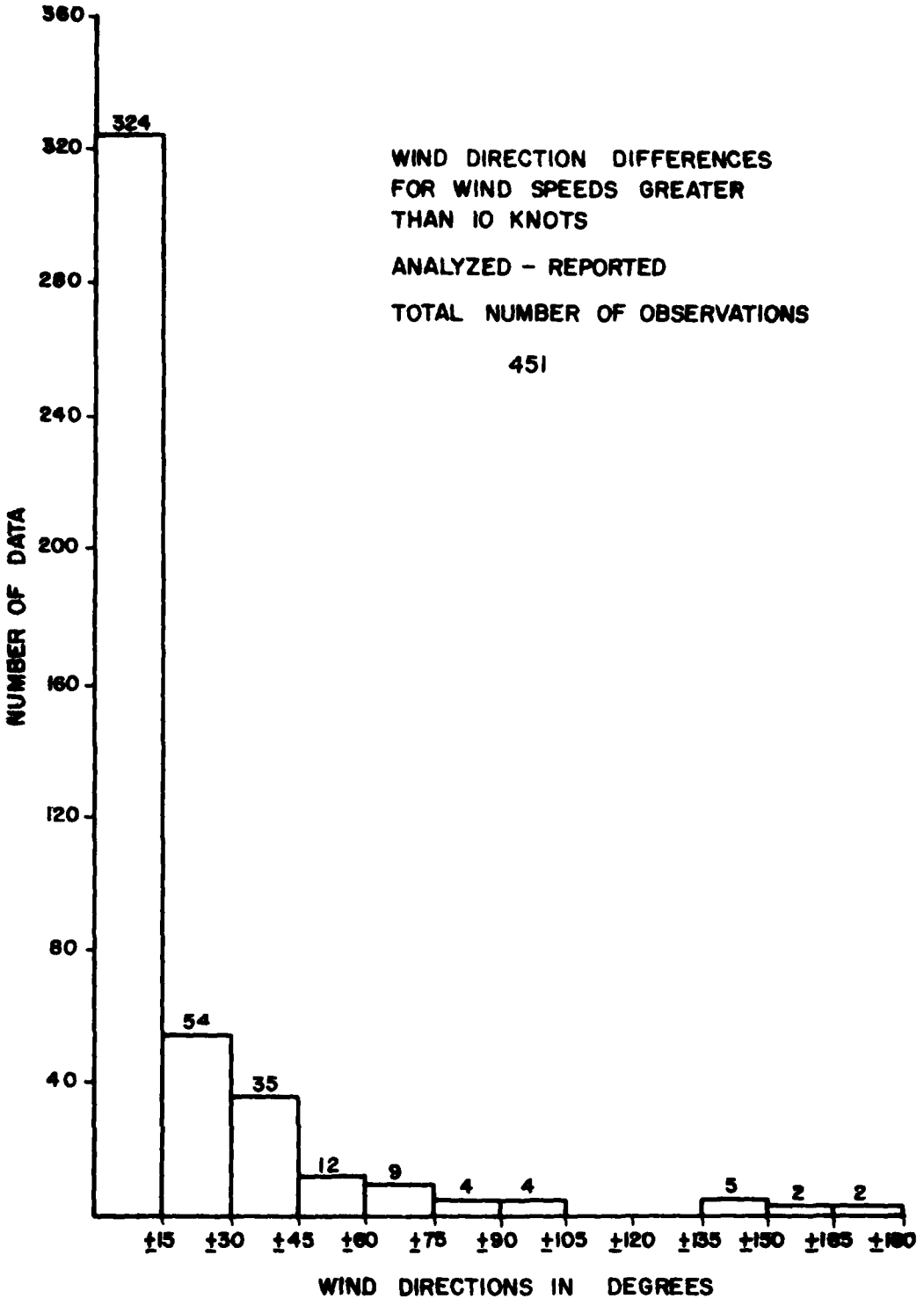
360
320
280
240
200
160
120
80
40
NUMBER OF DATA
324
54
35
12
9
4
4
5
2
2
±15
±30
±45
±60
±75
±90
±105
±120
±135
±150
±165
±180
WIND DIRECTIONS IN DEGREES
WIND DIRECTION DIFFERENCES
FOR WIND SPEEDS GREATER
THAN 10 KNOTS
ANALYZED - REPORTED
TOTAL NUMBER OF OBSERVATIONS
451

FIGURE 7

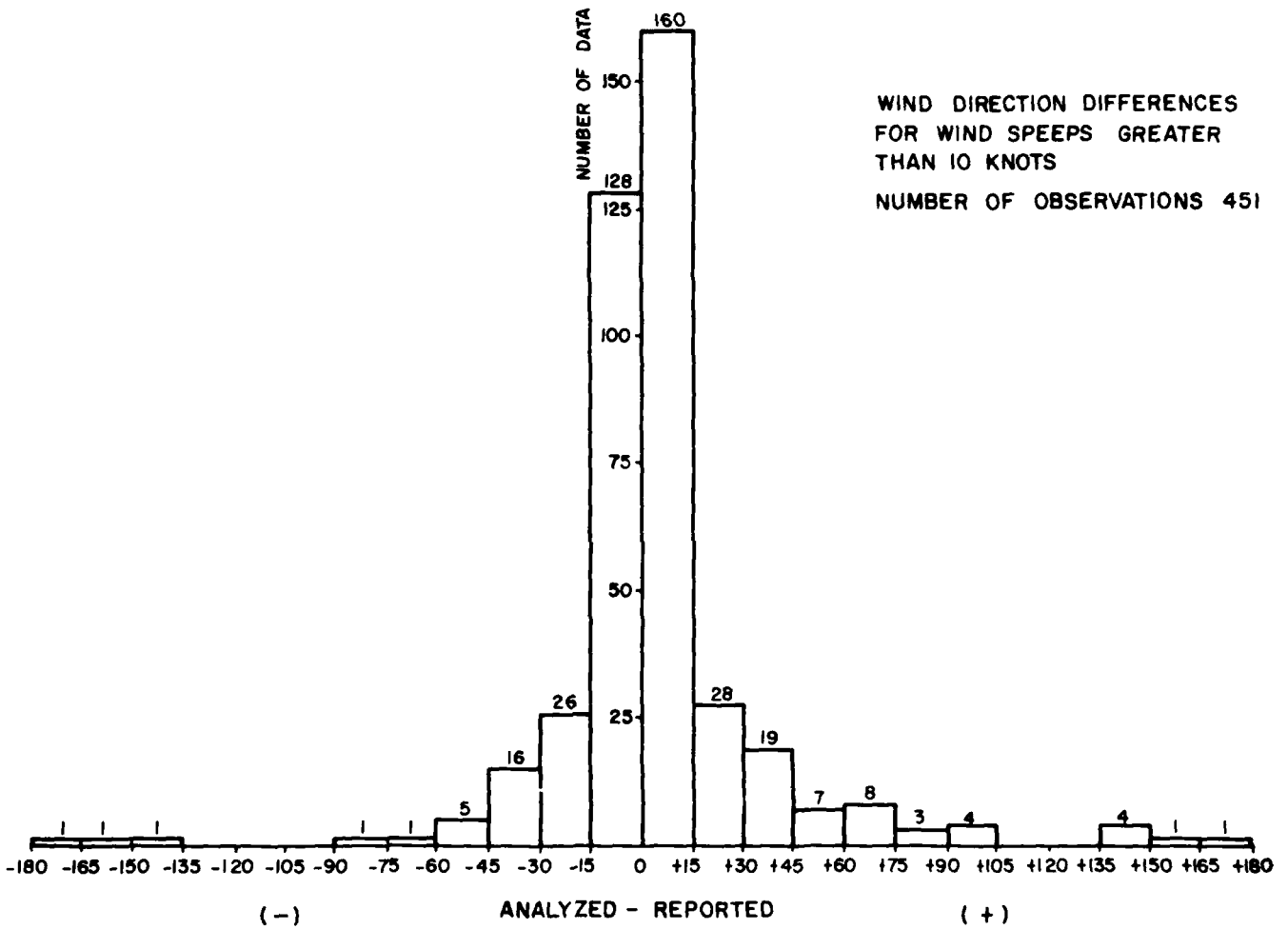

WIND DIRECTION DIFFERENCES
FOR WIND SPEEPS GREATER
THAN 10 KNOTS

NUMBER OF OBSERVATIONS 451

36 DATA HAD ZERO DIFFERENCE

FIGURE 8

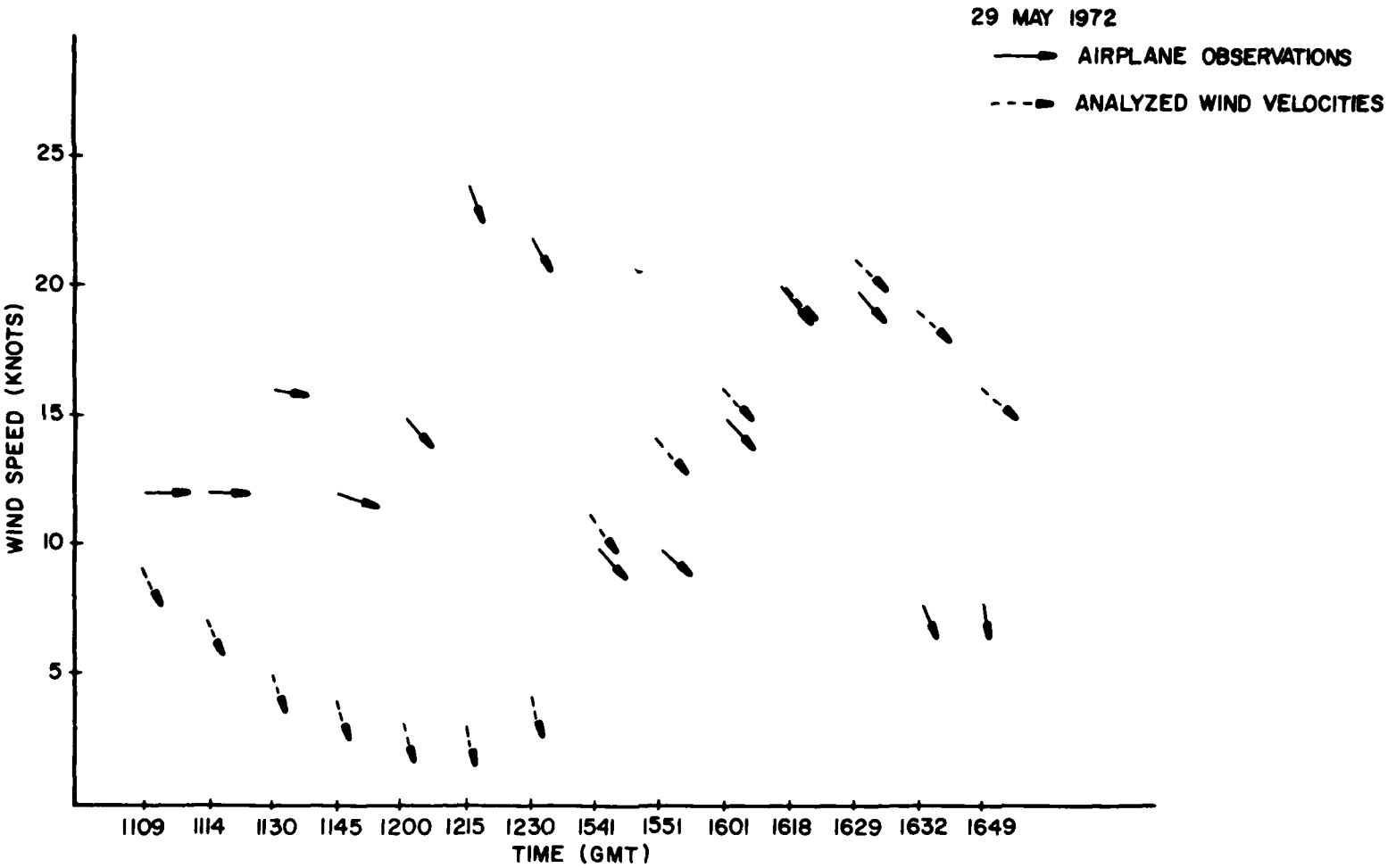

FIGURE 9

AIRPLANE WIND OBSERVATIONS VERSUS ANALYZED WIND VELOCITIES

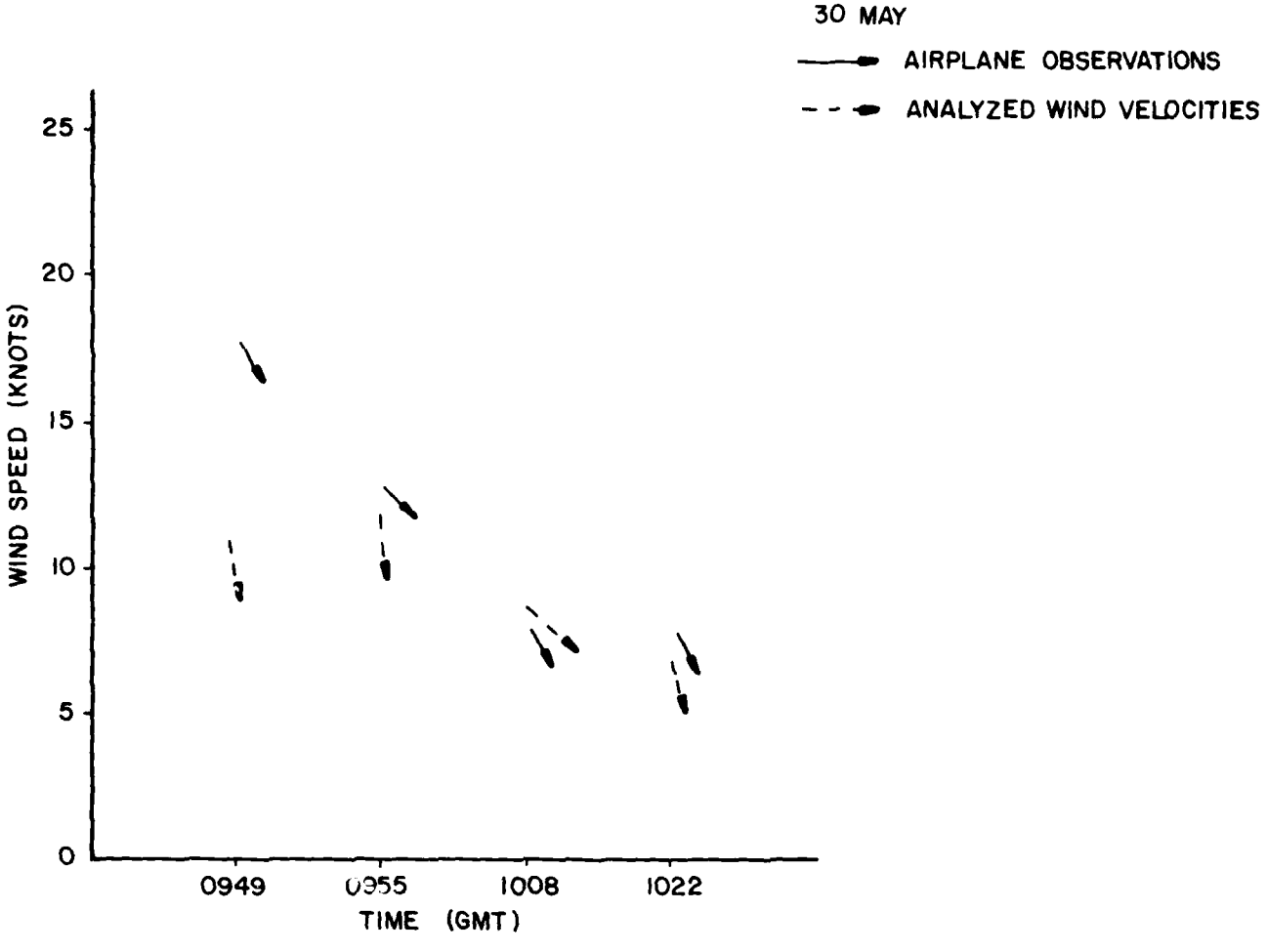

FIGURE 10

AIRPLANE WIND OBSERVATIONS VERSUS ANALYZED WIND VELOCITIES

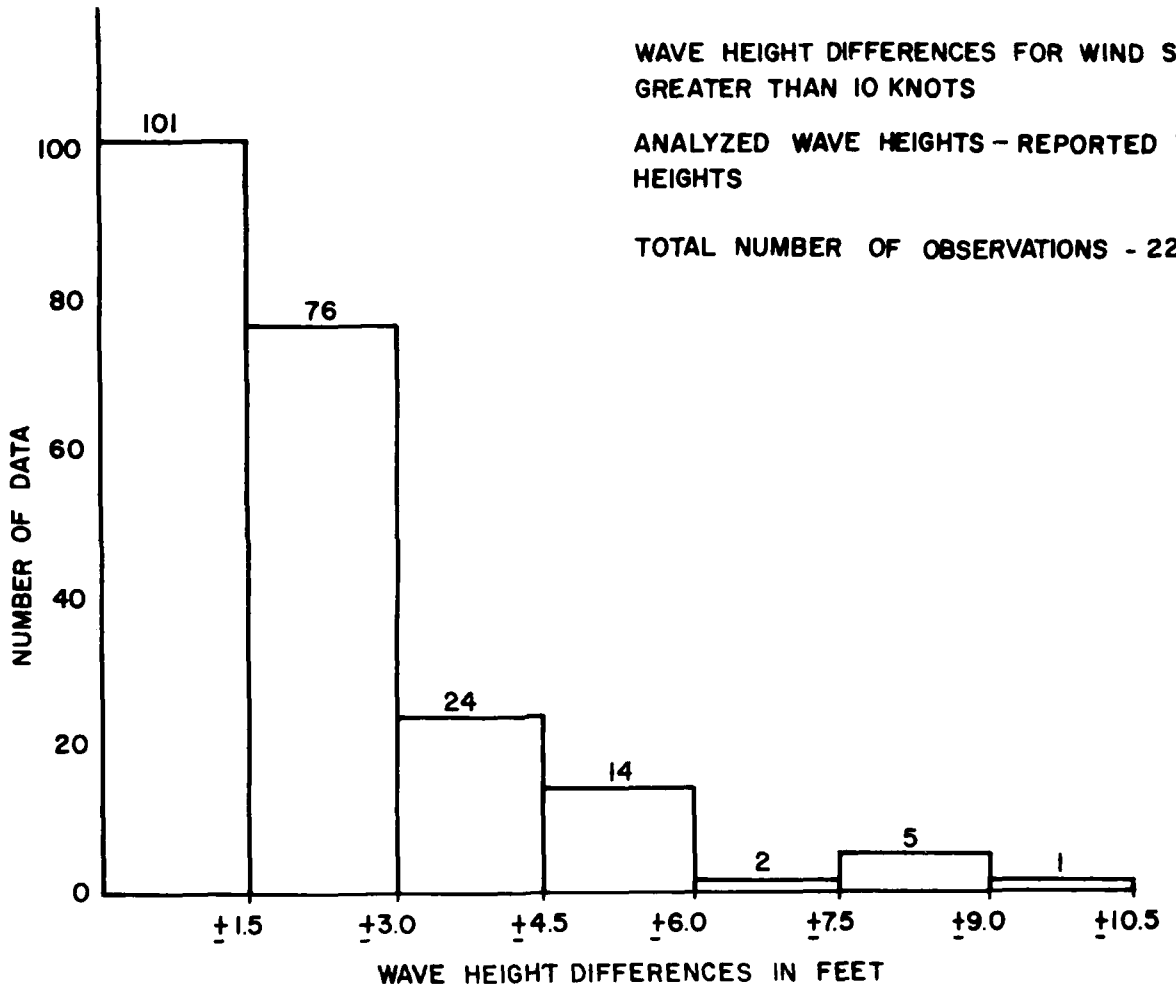
WAVE HEIGHT DIFFERENCES FOR WIND SPEEDS GREATER THAN 10 KNOTS
ANALYZED WAVE HEIGHTS – REPORTED WAVE HEIGHTS
TOTAL NUMBER OF OBSERVATIONS - 223
NUMBER OF DATA
0
20
40
60
80
100
101
76
24
14
2
5
1
±1.5
±3.0
±4.5
±6.0
±7.5
±9.0
±10.5
WAVE HEIGHT DIFFERENCES IN FEET

FIGURE 11

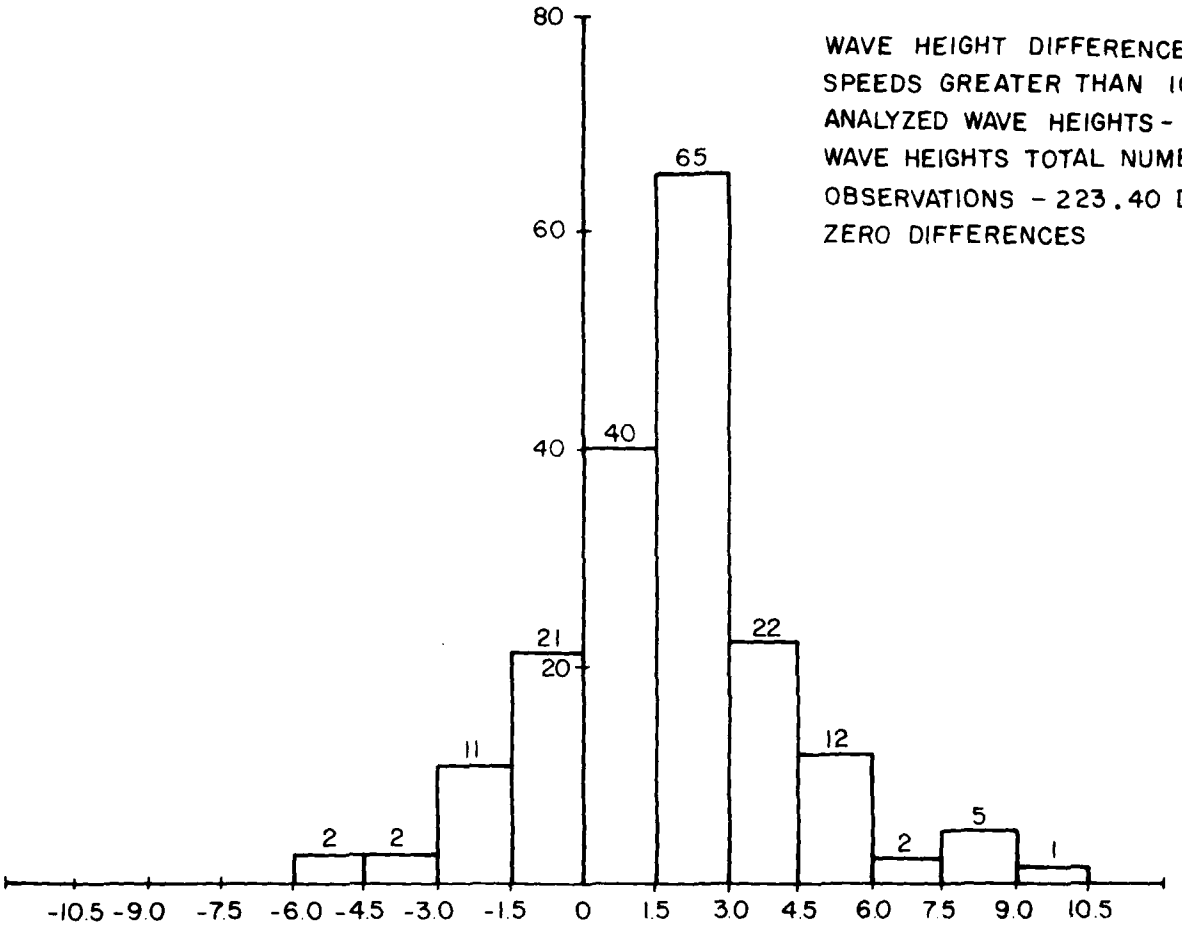
80
60
40
20
65
40
22
21
12
11
5
2
2
2
1
-10.5 -9.0 -7.5 -6.0 -4.5 -3.0 -1.5 0 1.5 3.0 4.5 6.0 7.5 9.0 10.5
WAVE HEIGHT DIFFERENCES FOR WIND SPEEDS GREATER THAN 10 KNOTS ANALYZED WAVE HEIGHTS - REPORTED WAVE HEIGHTS TOTAL NUMBER OF OBSERVATIONS - 223. 40 DATA HAD ZERO DIFFERENCES
WAVE HEIGHT DIFFERENCES IN FEET

FIGURE 12

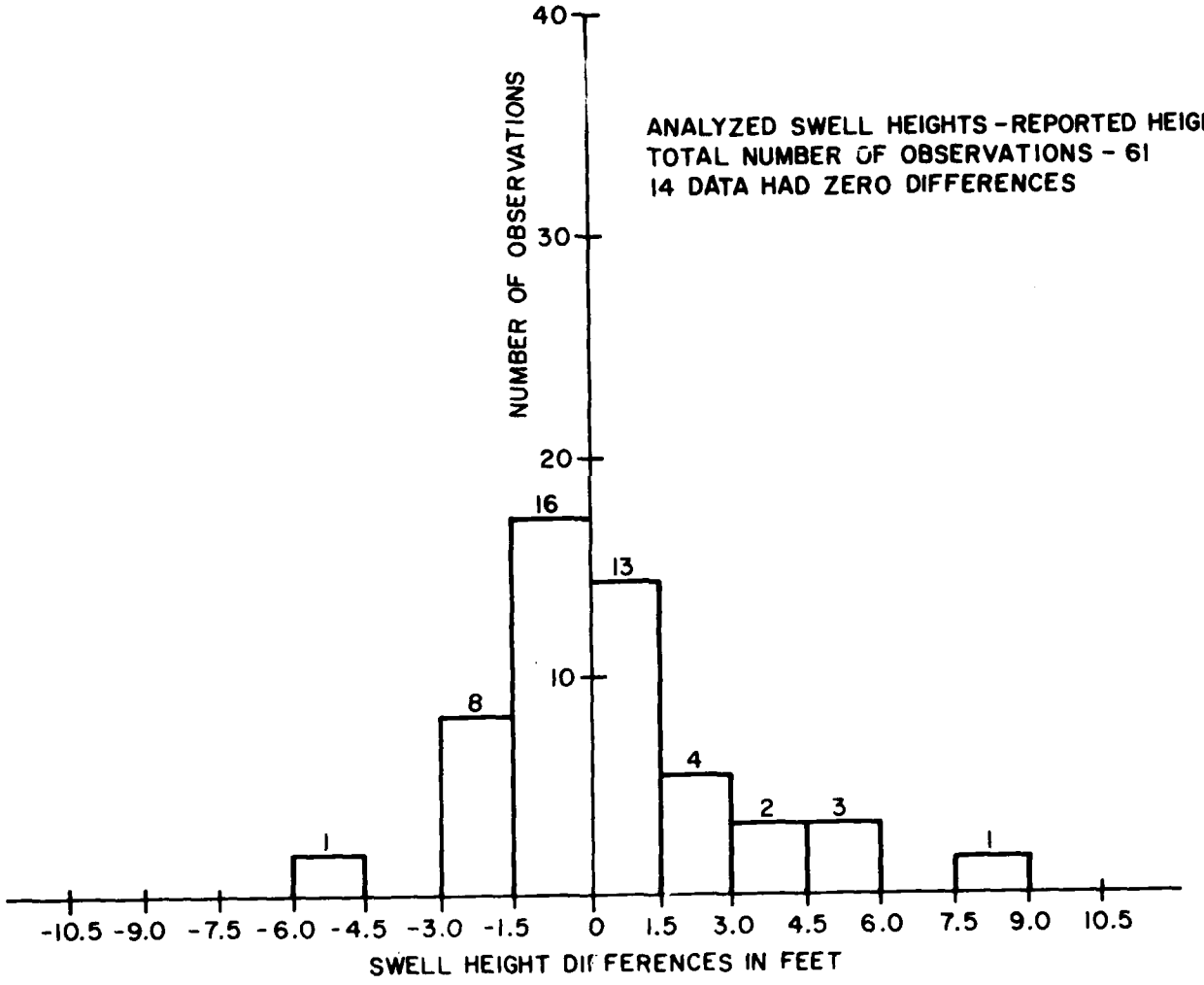
ANALYZED SWELL HEIGHTS - REPORTED HEIGHTS
TOTAL NUMBER OF OBSERVATIONS - 61
14 DATA HAD ZERO DIFFERENCES
NUMBER OF OBSERVATIONS
40
30
20
10
16
13
8
4
2
3
1
1
-10.5 -9.0 -7.5 -6.0 -4.5 -3.0 -1.5 0 1.5 3.0 4.5 6.0 7.5 9.0 10.5
SWELL HEIGHT DIFFERENCES IN FEET

Figure 13.

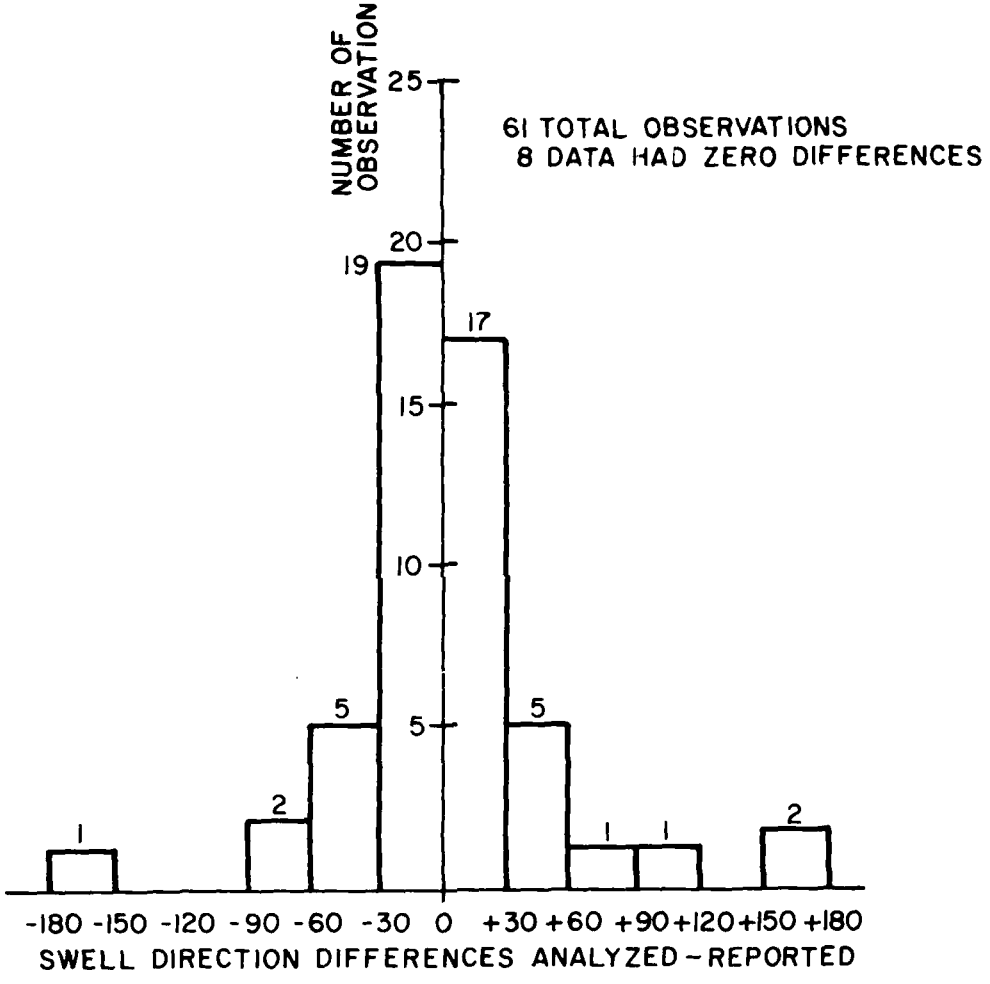
NUMBER OF OBSERVATION
25
20
15
10
5
61 TOTAL OBSERVATIONS
8 DATA HAD ZERO DIFFERENCES
19
17
5
5
2
1
1
1
2
-180 -150 -120 -90 -60 -30 0 +30 +60 +90 +120 +150 +180
SWELL DIRECTION DIFFERENCES ANALYZED - REPORTED

Figure 14.

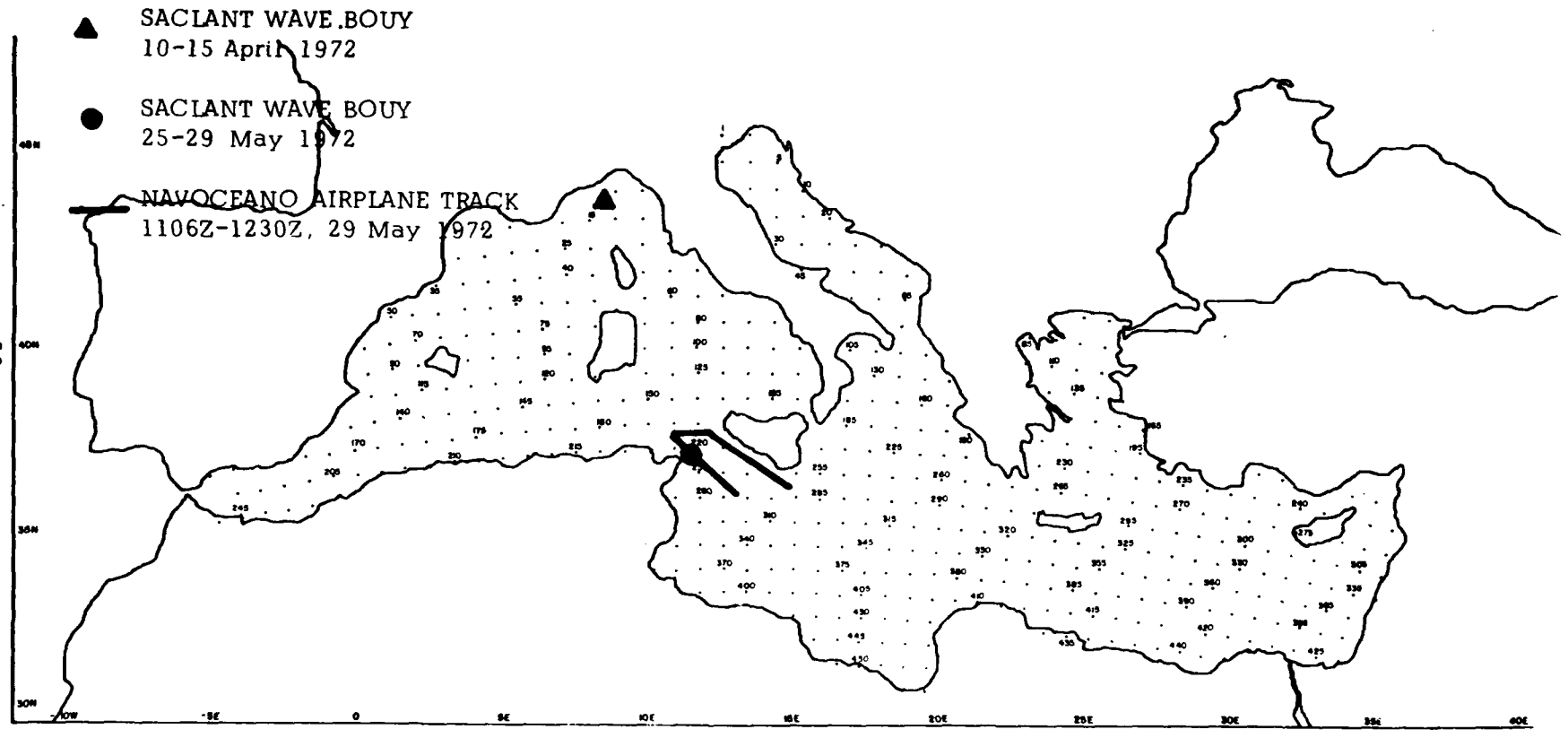

SACLANT WAVE BOUY EMPLANTMENT SITES AND NAVOCEANO AIRPANE TRACKS

FIGURE 15

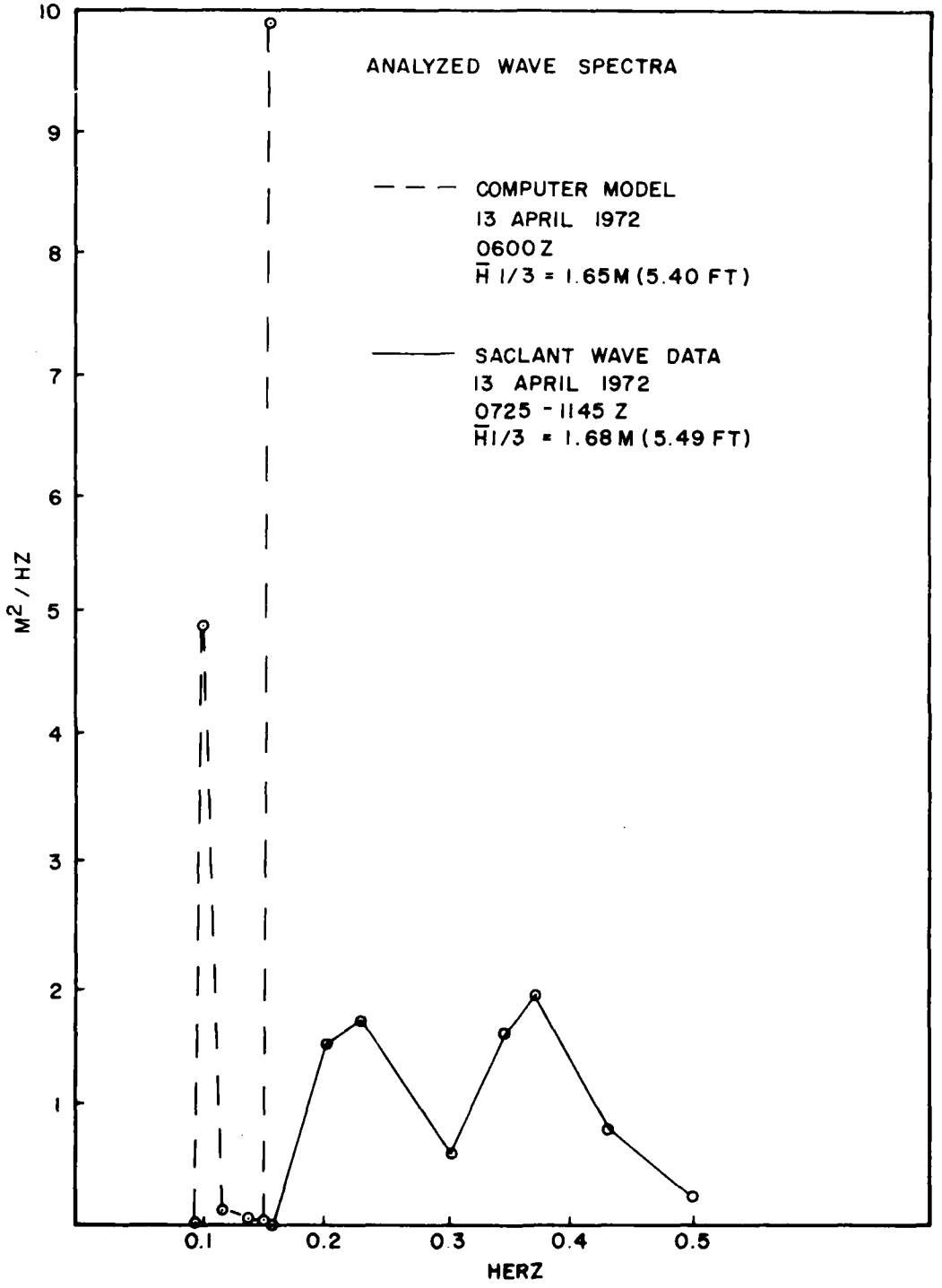
ANALYZED WAVE SPECTRA
COMPUTER MODEL
13 APRIL 1972
0600 Z
H̄ 1/3 = 1.65M (5.40 FT)
SACLANT WAVE DATA
13 APRIL 1972
0725 - 1145 Z
H̄1/3 = 1.68 M (5.49 FT)
M2 / HZ
HERZ
10
9
8
7
6
5
4
3
2
1
0.1
0.2
0.3
0.4
0.5

FIGURE 16

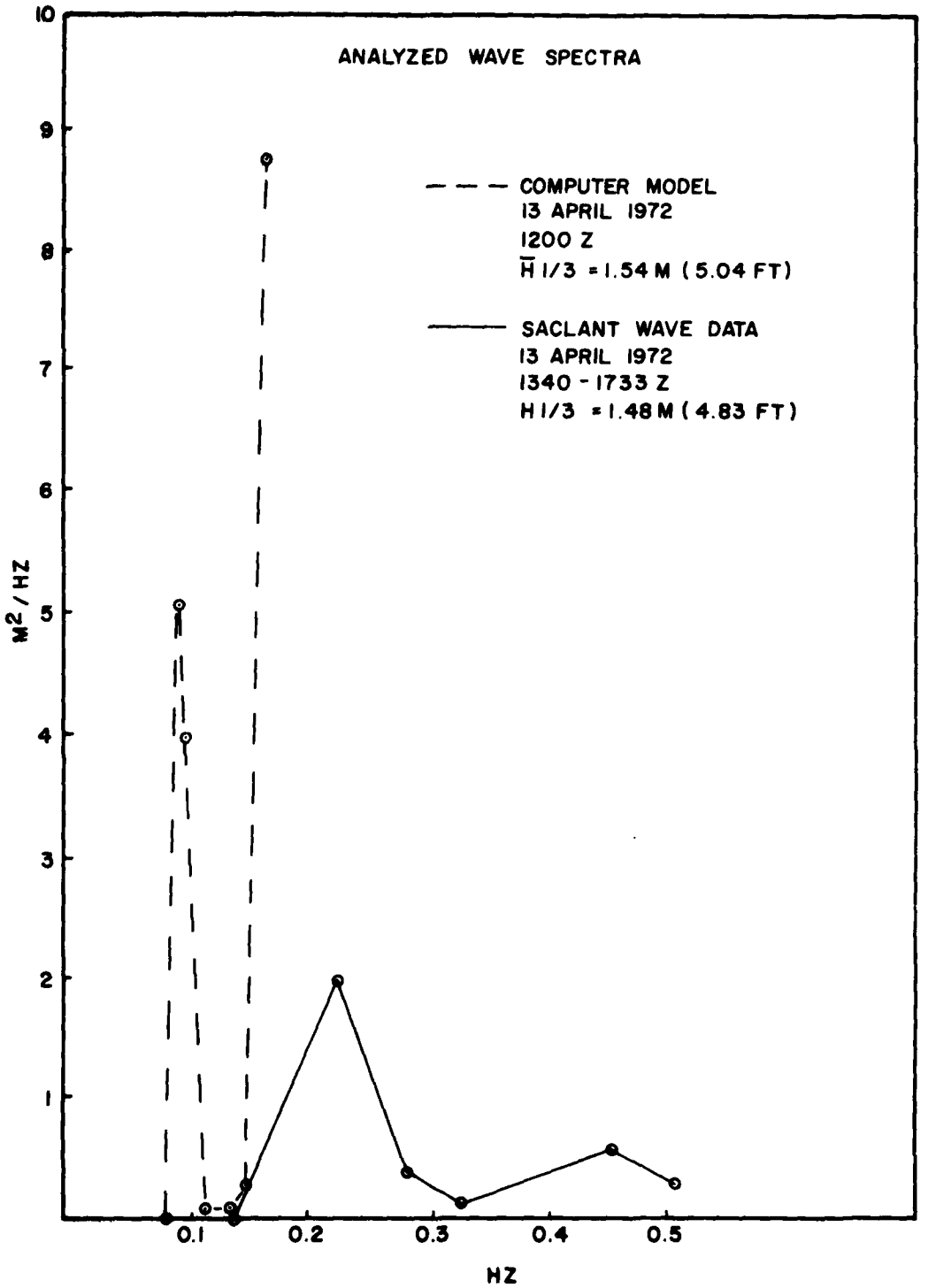
ANALYZED WAVE SPECTRA
COMPUTER MODEL
13 APRIL 1972
1200 Z
H̄ 1/3 = 1.54 M (5.04 FT)
SACLANT WAVE DATA
13 APRIL 1972
1340 - 1733 Z
H 1/3 = 1.48 M (4.83 FT)
M2 / HZ
HZ
10
9
8
7
6
5
4
3
2
1
0.1
0.2
0.3
0.4
0.5

FIGURE 17

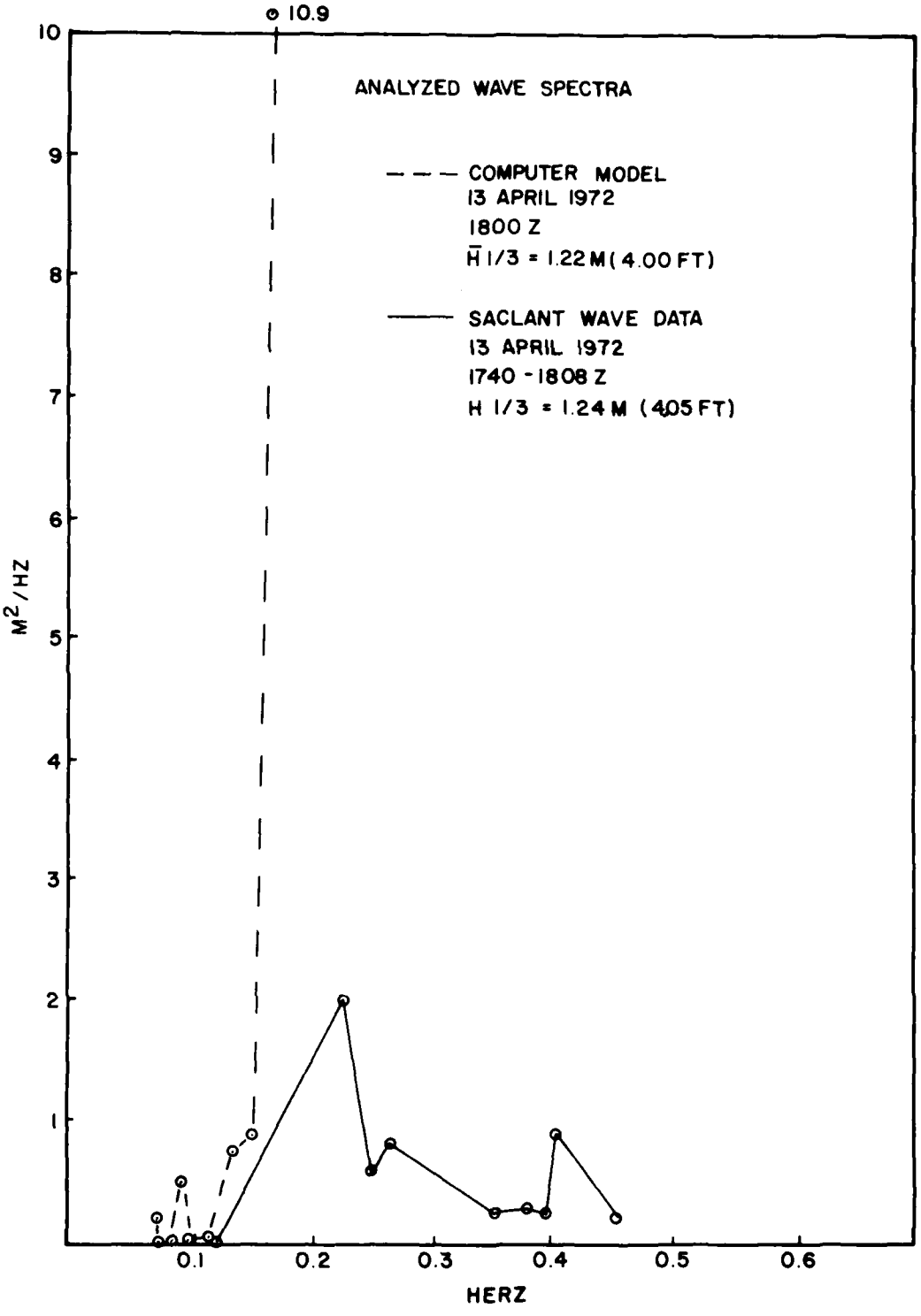
10.9
ANALYZED WAVE SPECTRA
COMPUTER MODEL
13 APRIL 1972
1800 Z
H̄ 1/3 = 1.22 M (4.00 FT)
SACLANT WAVE DATA
13 APRIL 1972
1740 - 1808 Z
H 1/3 = 1.24 M (4.05 FT)
M²/HZ
HERZ
10
9
8
7
6
5
4
3
2
1
0.1
0.2
0.3
0.4
0.5
0.6

FIGURE 18

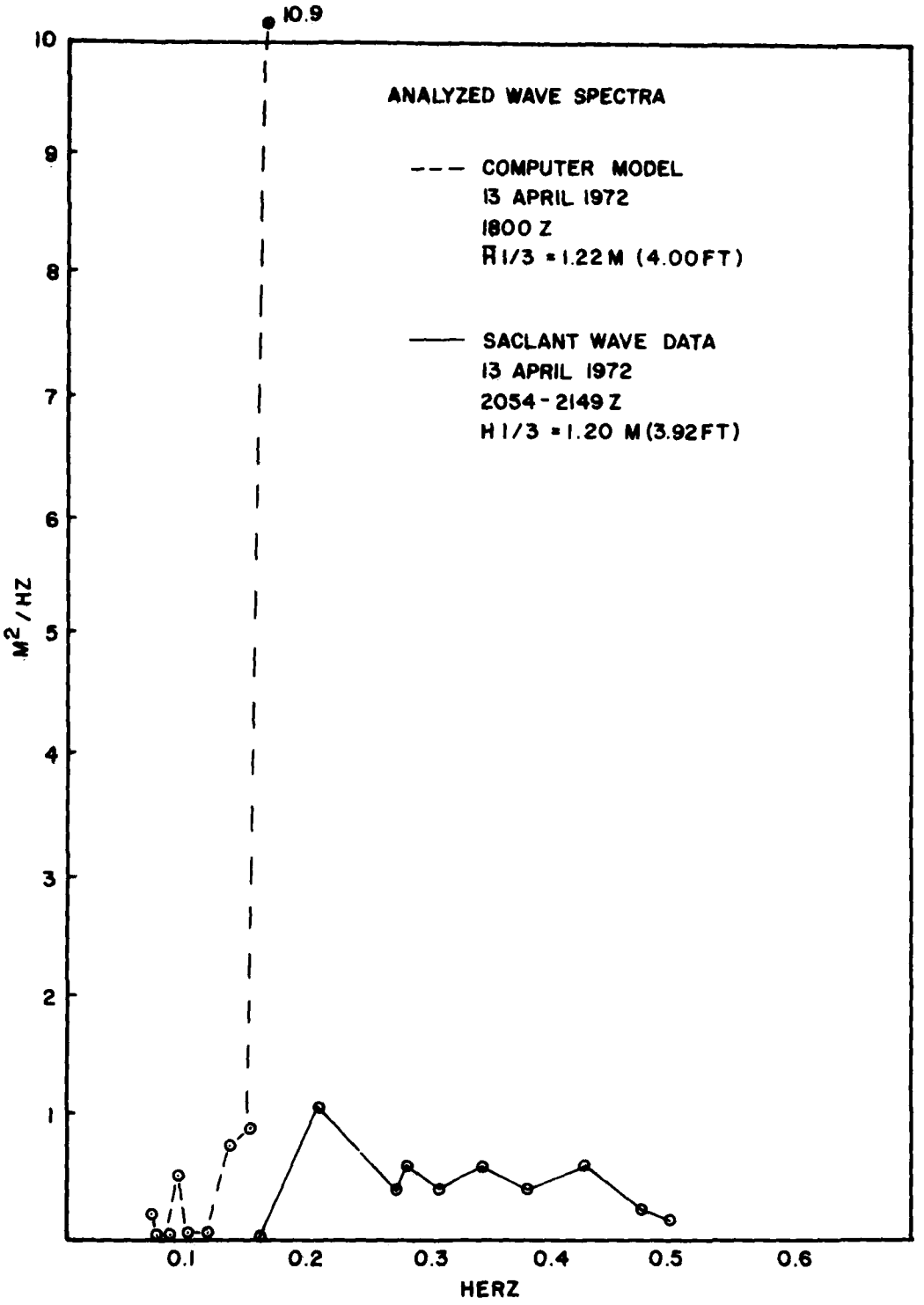
10.9
ANALYZED WAVE SPECTRA
--- COMPUTER MODEL
13 APRIL 1972
1800 Z
H1/3 = 1.22 M (4.00FT)
—— SACLANT WAVE DATA
13 APRIL 1972
2054 - 2149 Z
H 1/3 = 1.20 M (3.92FT)
M²/HZ
HERZ
0.1
0.2
0.3
0.4
0.5
0.6
1
2
3
4
5
6
7
8
9
10

FIGURE 19

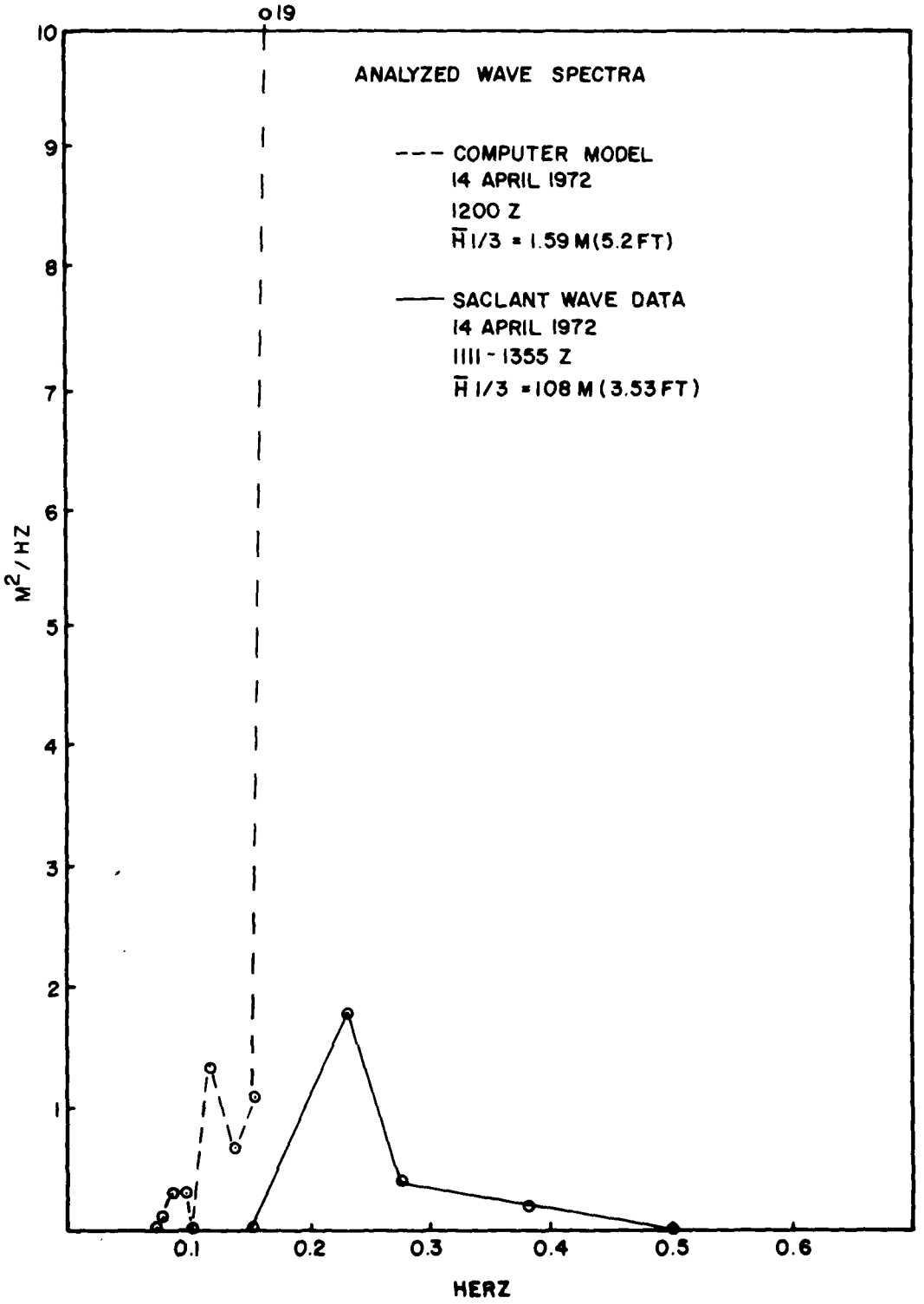
o19
ANALYZED WAVE SPECTRA
--- COMPUTER MODEL
14 APRIL 1972
1200 Z
H̄ 1/3 = 1.59 M(5.2 FT)
—— SACLANT WAVE DATA
14 APRIL 1972
1111 - 1355 Z
H̄ 1/3 = 108 M (3.53 FT)
M²/HZ
HERZ
10
9
8
7
6
5
4
3
2
1
0.1
0.2
0.3
0.4
0.5
0.6

FIGURE 20

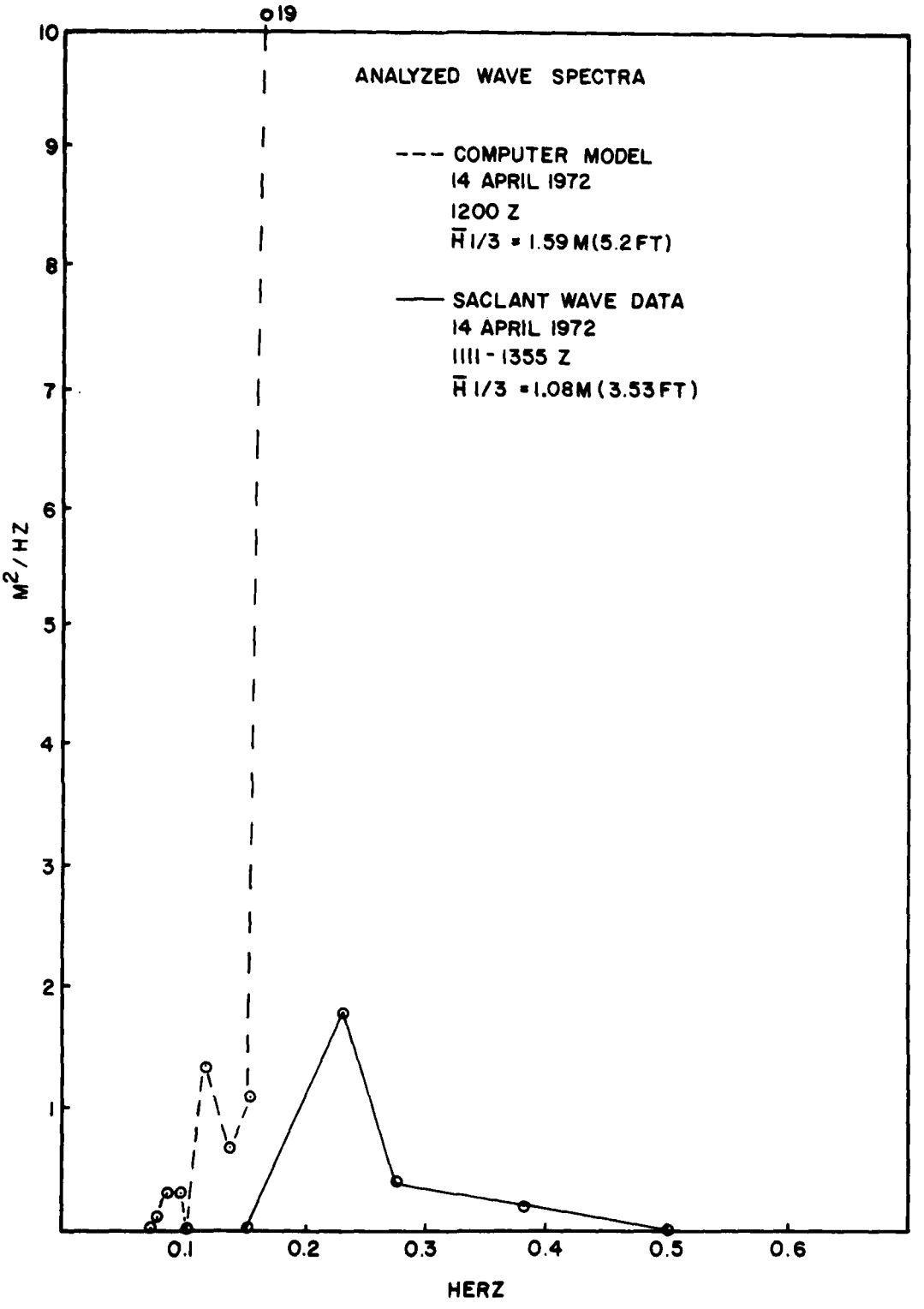
o19
ANALYZED WAVE SPECTRA
--- COMPUTER MODEL
14 APRIL 1972
1200 Z
$\bar{H}$ 1/3 = 1.59 M(5.2 FT)
—— SACLANT WAVE DATA
14 APRIL 1972
1111 - 1355 Z
$\bar{H}$ 1/3 = 1.08M (3.53 FT)
M^2/HZ
10
9
8
7
6
5
4
3
2
1
0.1
0.2
0.3
0.4
0.5
0.6
HERZ

FIGURE 21

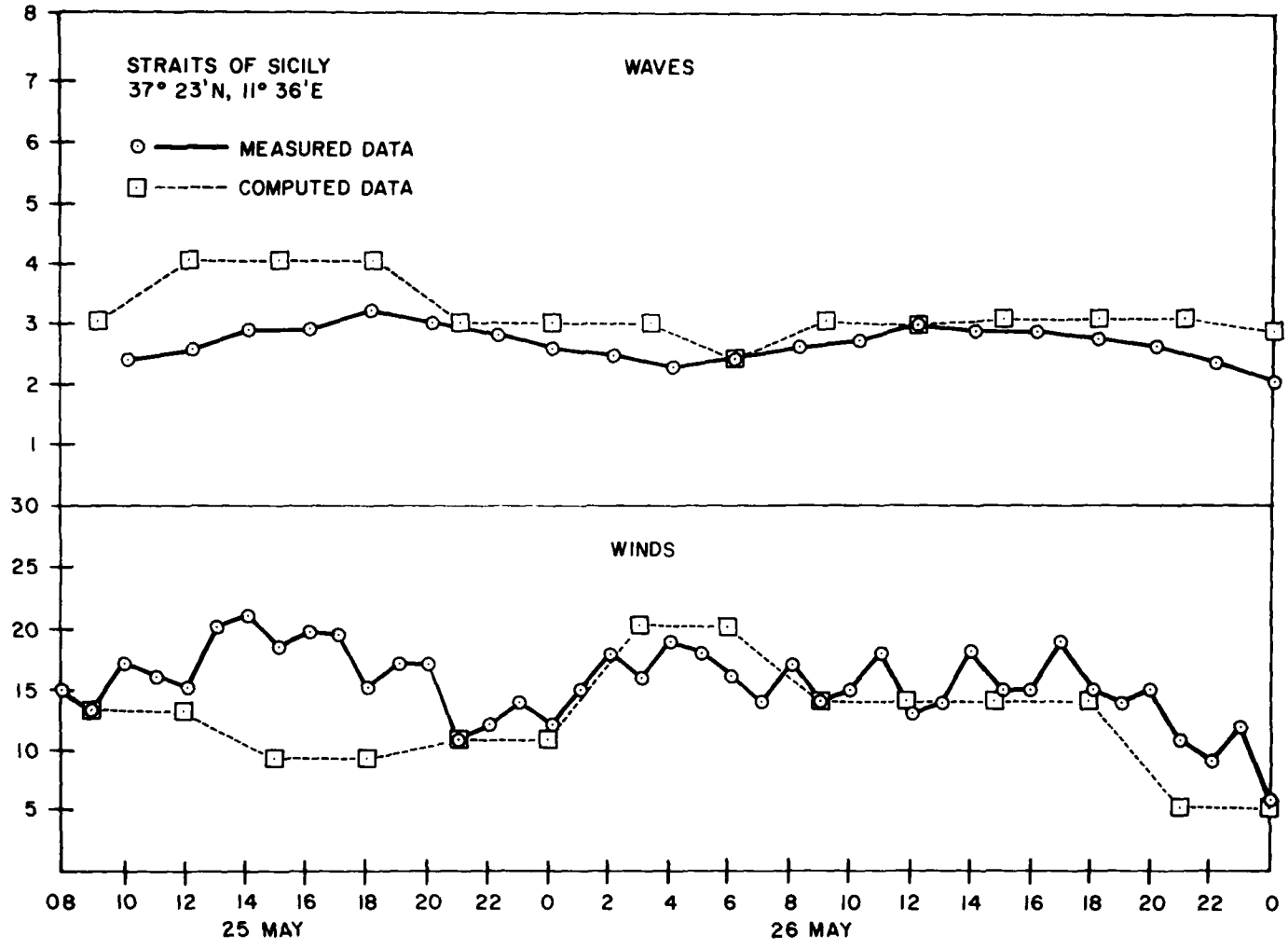
STRAITS OF SICILY
37° 23'N, 11° 36'E
WAVES
MEASURED DATA
COMPUTED DATA
WINDS
8
7
6
5
4
3
2
1
30
25
20
15
10
5
08 10 12 14 16 18 20 22 0 2 4 6 8 10 12 14 16 18 20 22 0
25 MAY
26 MAY

Figure 22.

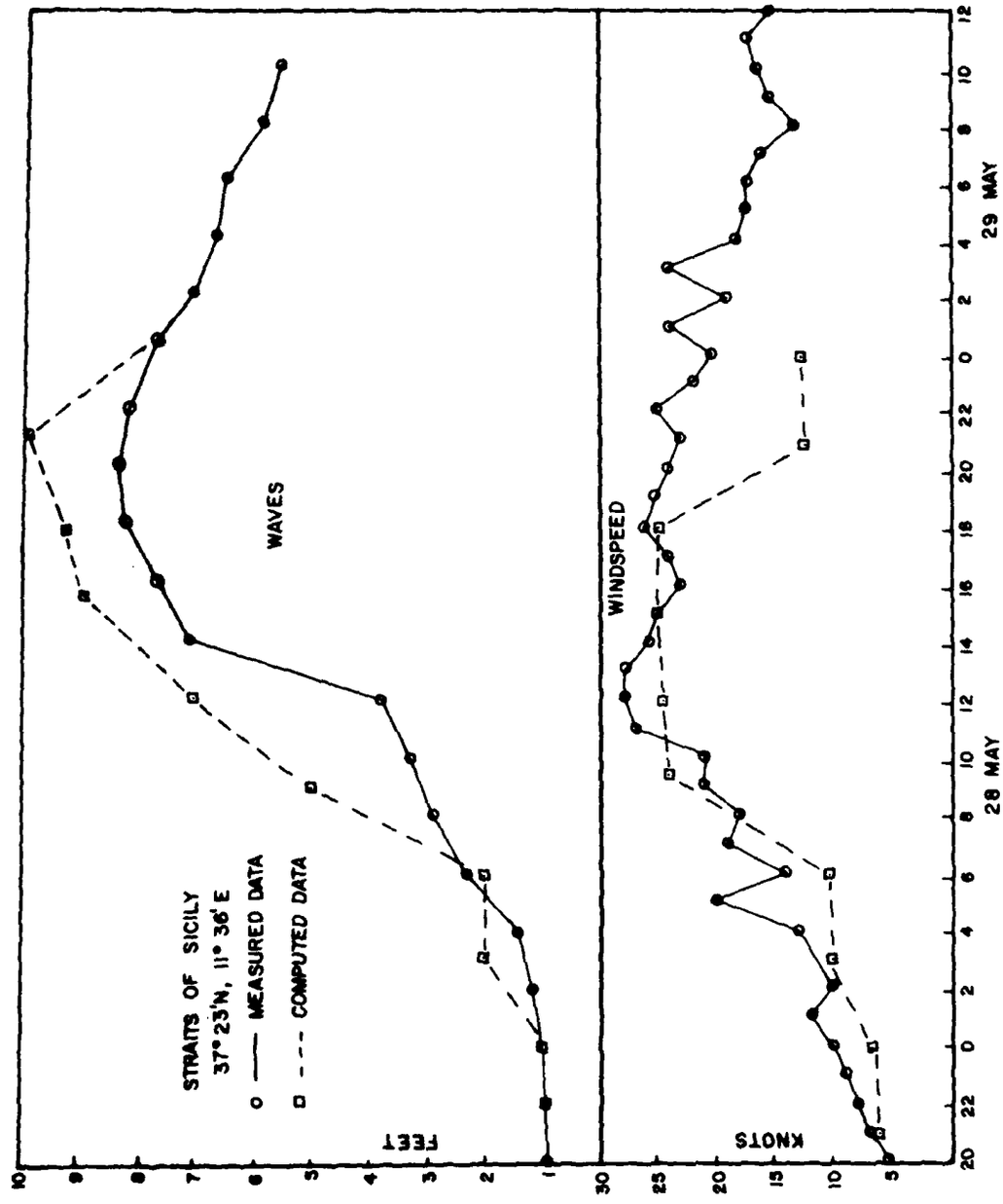
STRAITS OF SICILY
37° 23'N, 11° 36'E
MEASURED DATA
COMPUTED DATA
WAVES
FEET
WINDSPEED
KNOTS
28 MAY
29 MAY

FIGURE 23

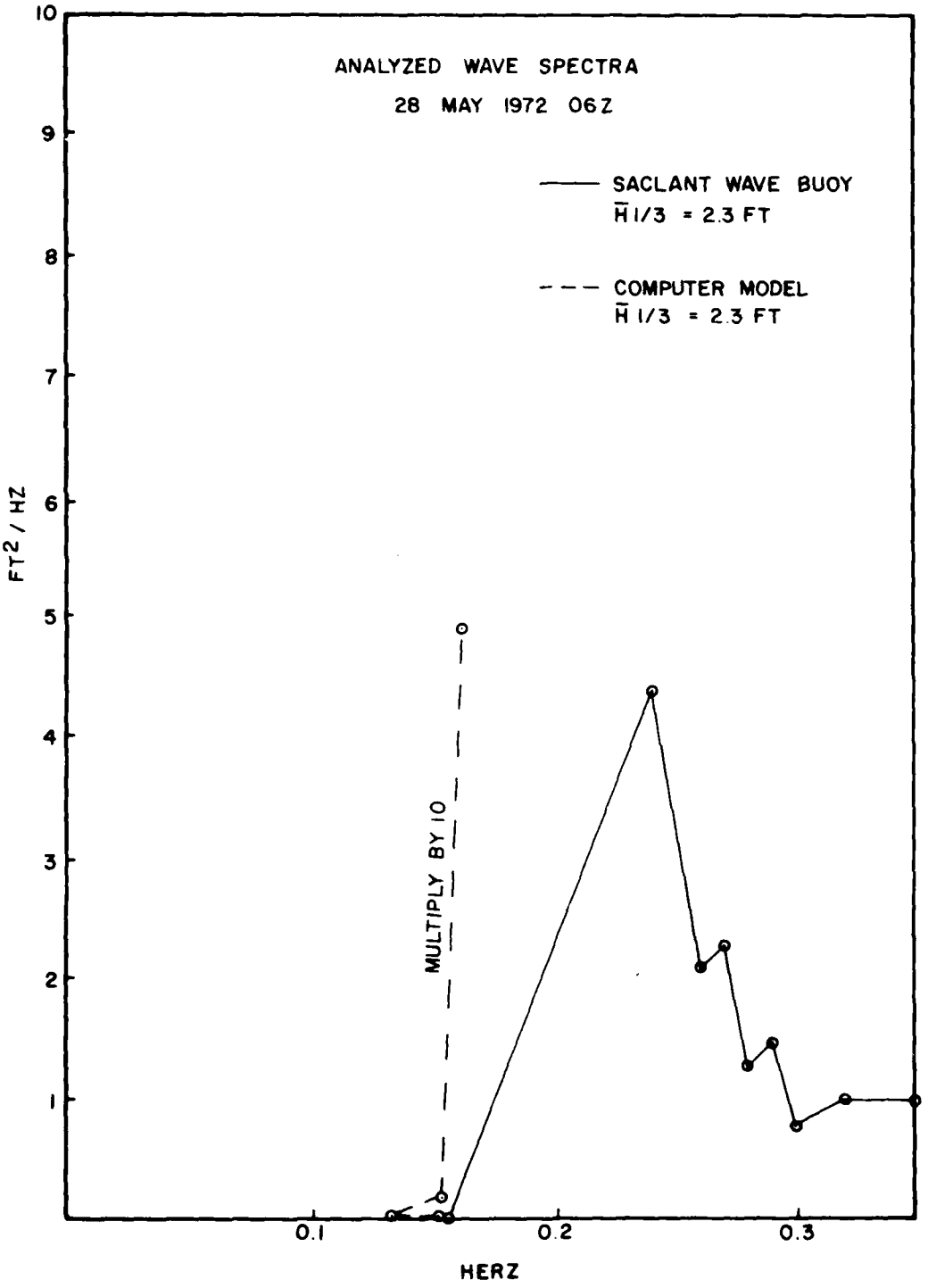
ANALYZED WAVE SPECTRA
28 MAY 1972 06Z
SACLANT WAVE BUOY
H̄1/3 = 2.3 FT
COMPUTER MODEL
H̄1/3 = 2.3 FT
MULTIPLY BY 10
FT2 / HZ
HERZ
10
9
8
7
6
5
4
3
2
1
0.1
0.2
0.3

FIGURE 24

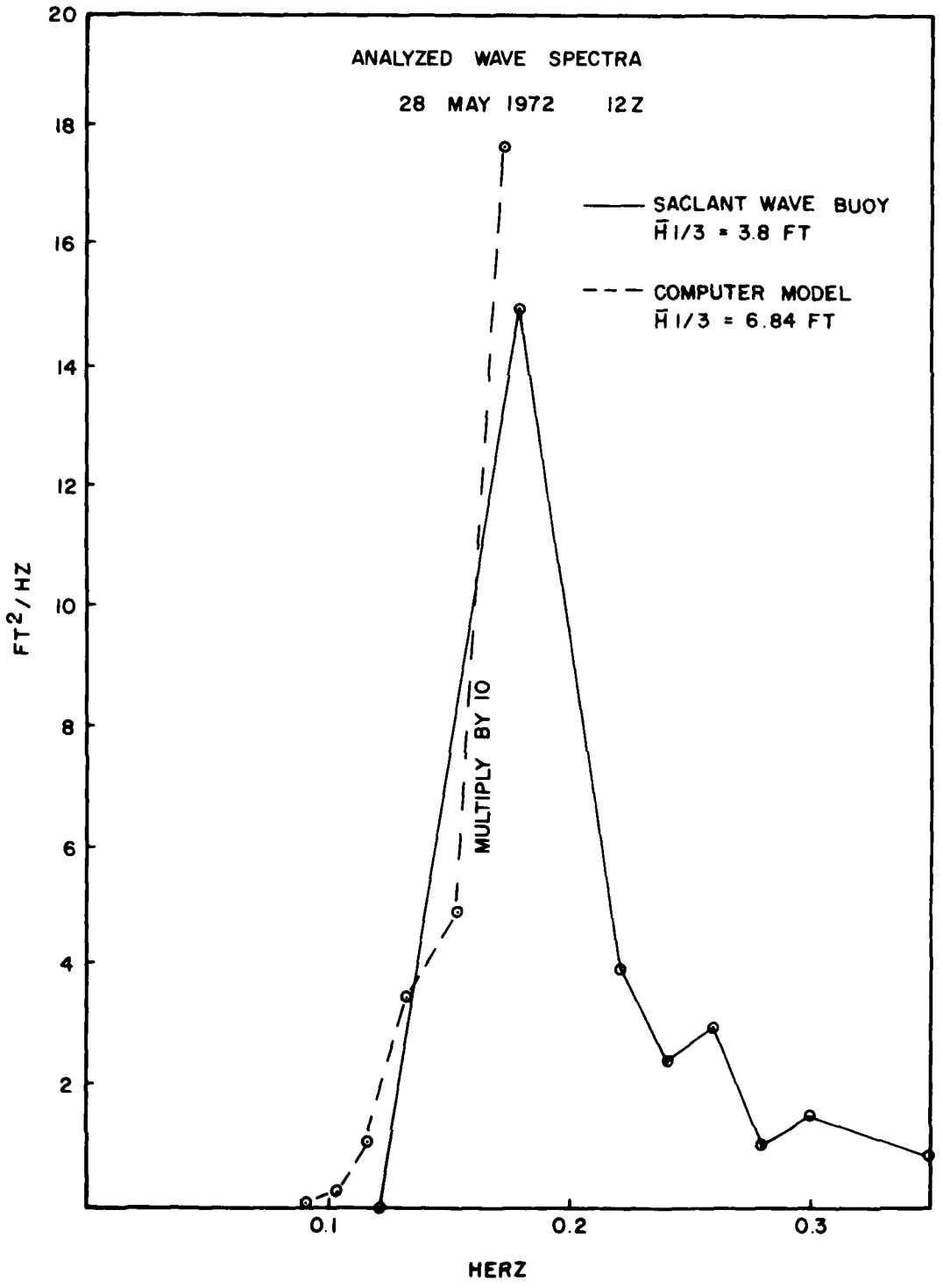
ANALYZED WAVE SPECTRA
28 MAY 1972 12Z
SACLANT WAVE BUOY
H̄1/3 = 3.8 FT
COMPUTER MODEL
H̄1/3 = 6.84 FT
MULTIPLY BY 10
FT²/HZ
HERZ
20
18
16
14
12
10
8
6
4
2
0.1
0.2
0.3

FIGURE 25

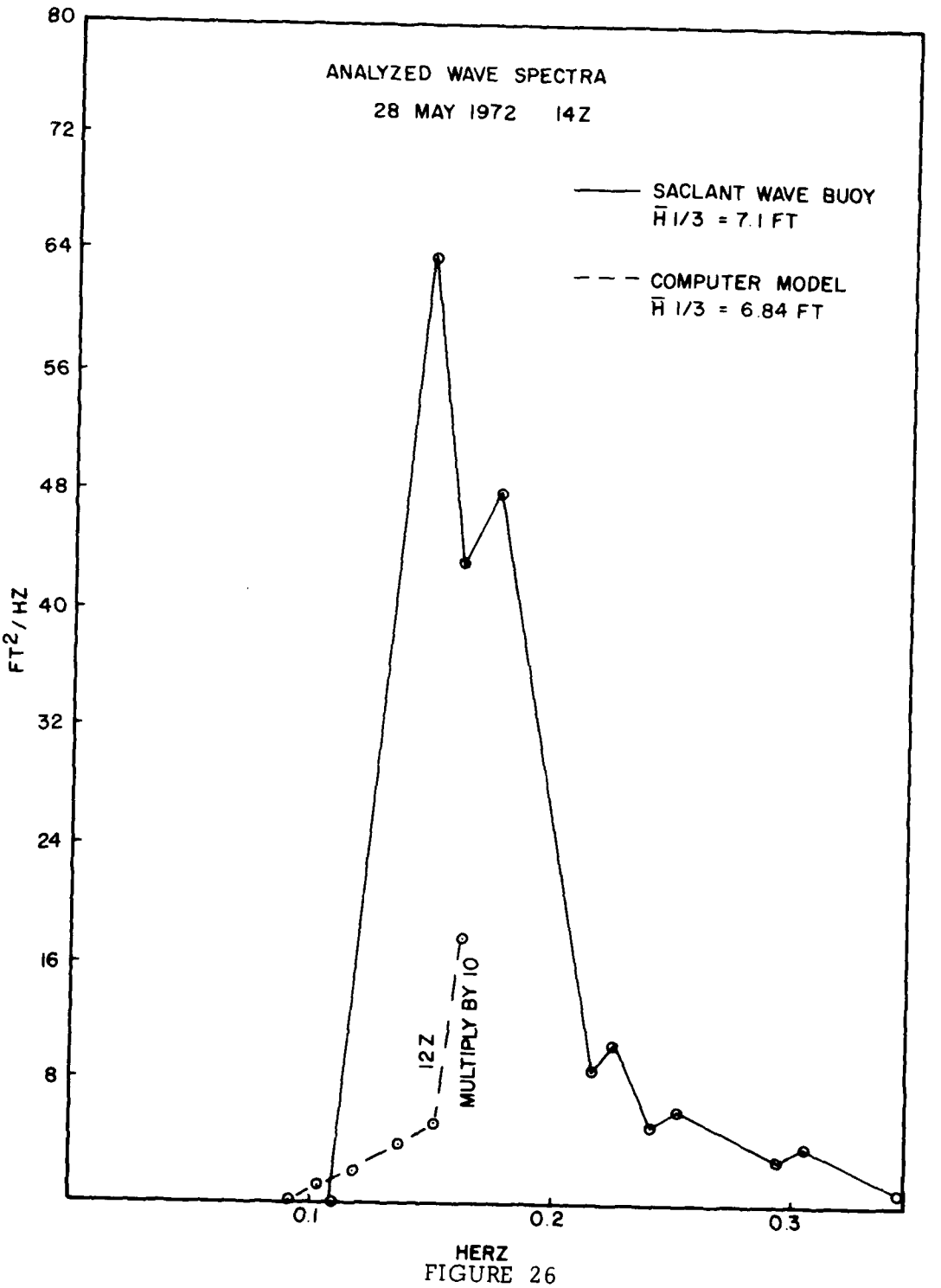
ANALYZED WAVE SPECTRA
28 MAY 1972 14Z
SACLANT WAVE BUOY
H̄ 1/3 = 7.1 FT
COMPUTER MODEL
H̄ 1/3 = 6.84 FT
12Z
MULTIPLY BY 10
FT²/HZ
HERZ
80
72
64
56
48
40
32
24
16
8
0.1
0.2
0.3

FIGURE 26

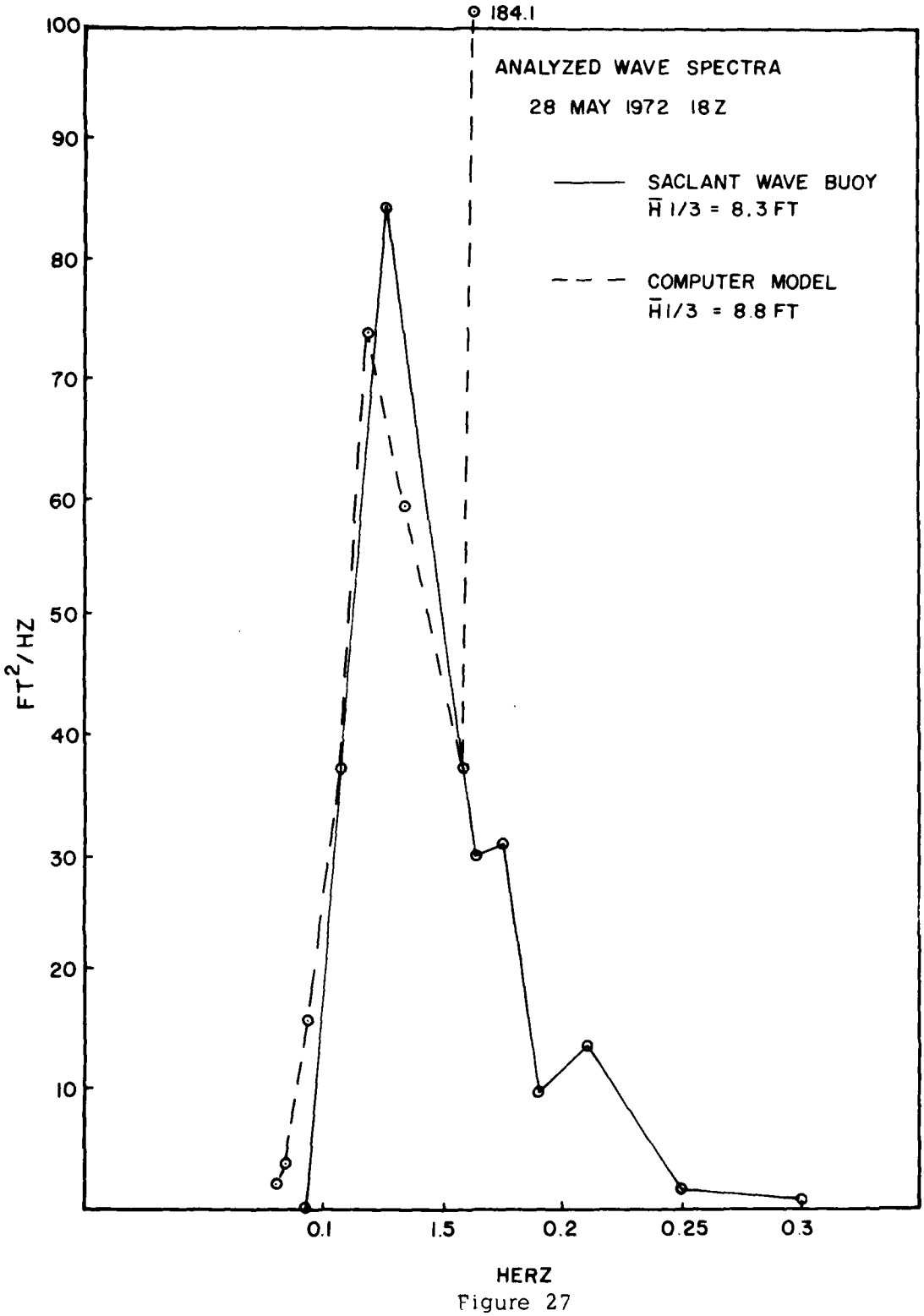
184.1
ANALYZED WAVE SPECTRA
28 MAY 1972 18Z
SACLANT WAVE BUOY
H̄ 1/3 = 8.3 FT
COMPUTER MODEL
H̄1/3 = 8.8 FT
100
90
80
70
60
50
40
30
20
10
FT²/HZ
0.1
1.5
0.2
0.25
0.3
HERZ

Figure 27

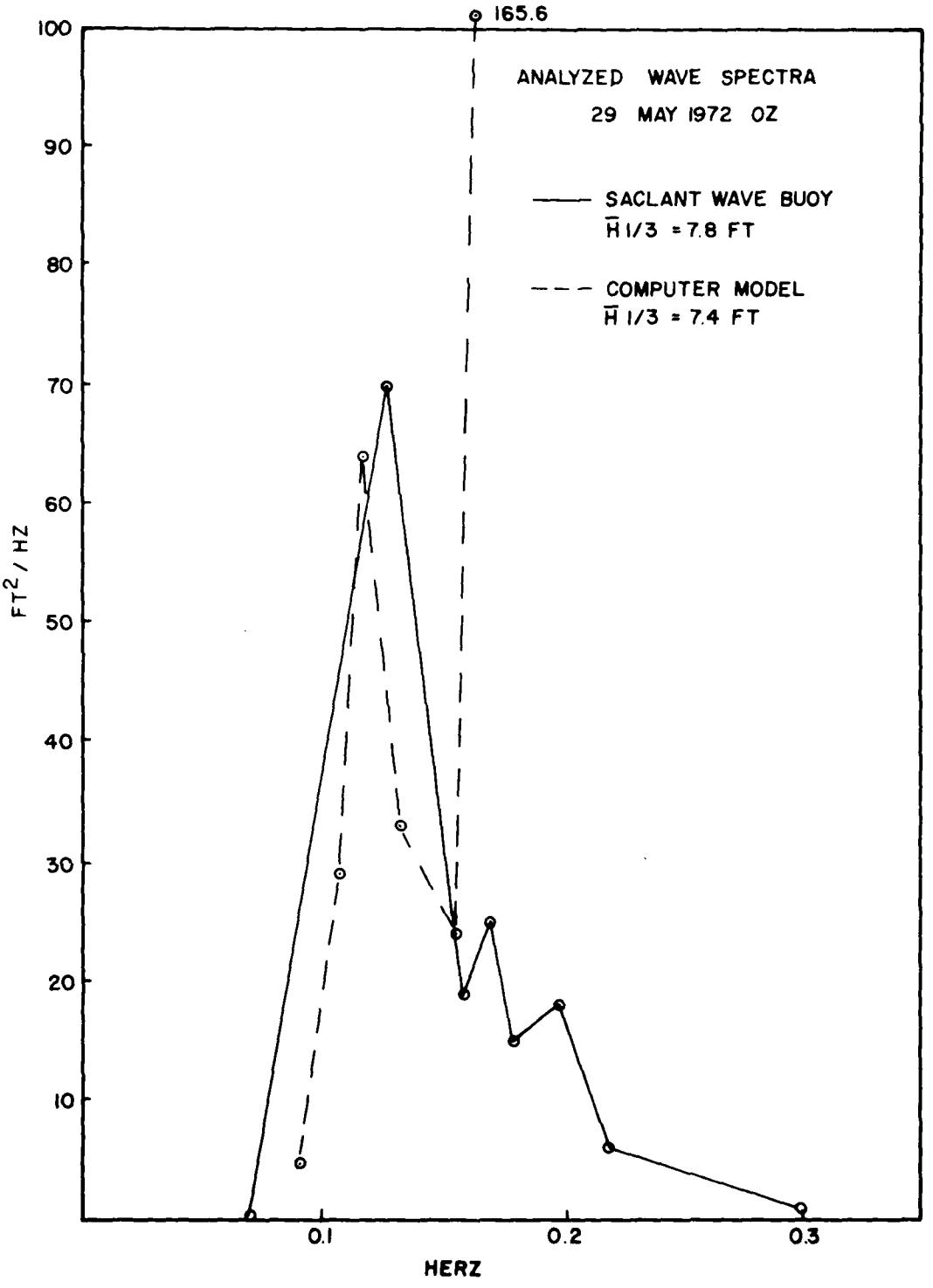
165.6
ANALYZED WAVE SPECTRA
29 MAY 1972 0Z
SACLANT WAVE BUOY
H̄ 1/3 = 7.8 FT
COMPUTER MODEL
H̄ 1/3 = 7.4 FT
100
90
80
70
60
50
40
30
20
10
FT²/HZ
0.1
0.2
0.3
HERZ

FIGURE 28

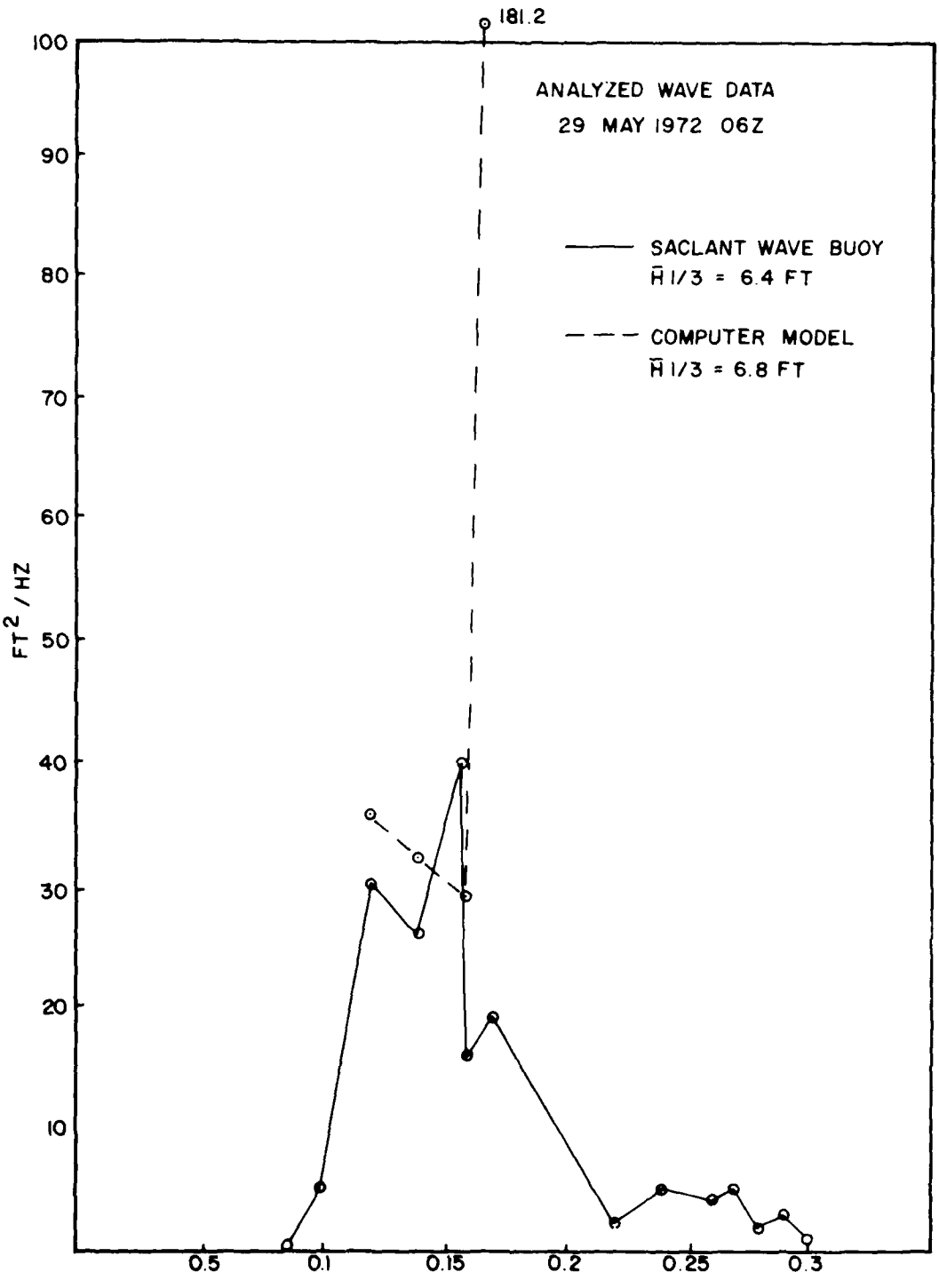
181.2
ANALYZED WAVE DATA
29 MAY 1972 06Z
SACLANT WAVE BUOY
H̄ 1/3 = 6.4 FT
COMPUTER MODEL
H̄ 1/3 = 6.8 FT
FT² / HZ
100
90
80
70
60
50
40
30
20
10
0.5
0.1
0.15
0.2
0.25
0.3

FIGURE 29

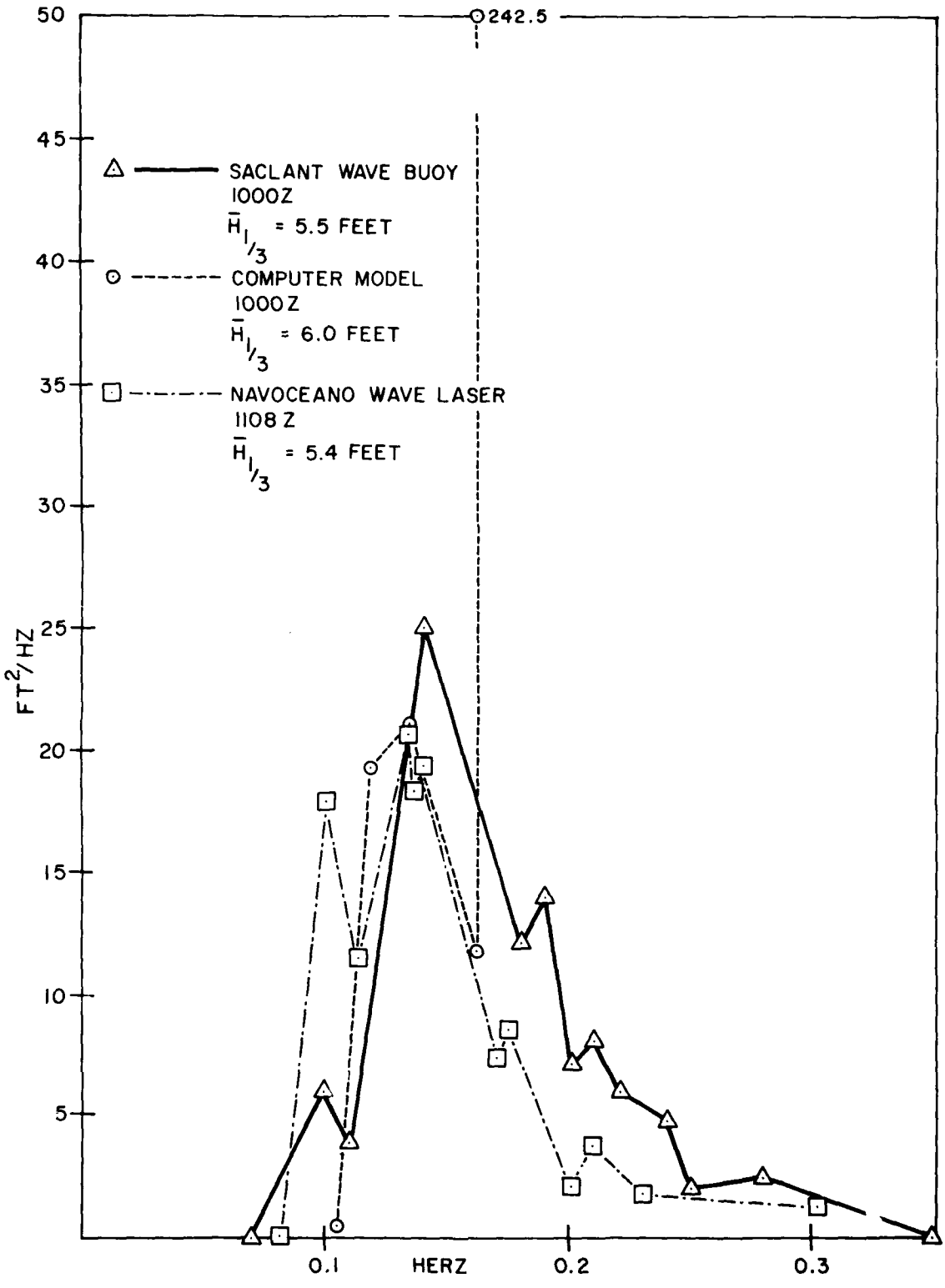
50
45
40
35
30
25
20
15
10
5
242.5
SACLANT WAVE BUOY
1000Z
$\bar{H}_{1/3}$ = 5.5 FEET
COMPUTER MODEL
1000Z
$\bar{H}_{1/3}$ = 6.0 FEET
NAVOCEANO WAVE LASER
1108Z
$\bar{H}_{1/3}$ = 5.4 FEET
FT²/HZ
0.1
HERZ
0.2
0.3

Figure 30.

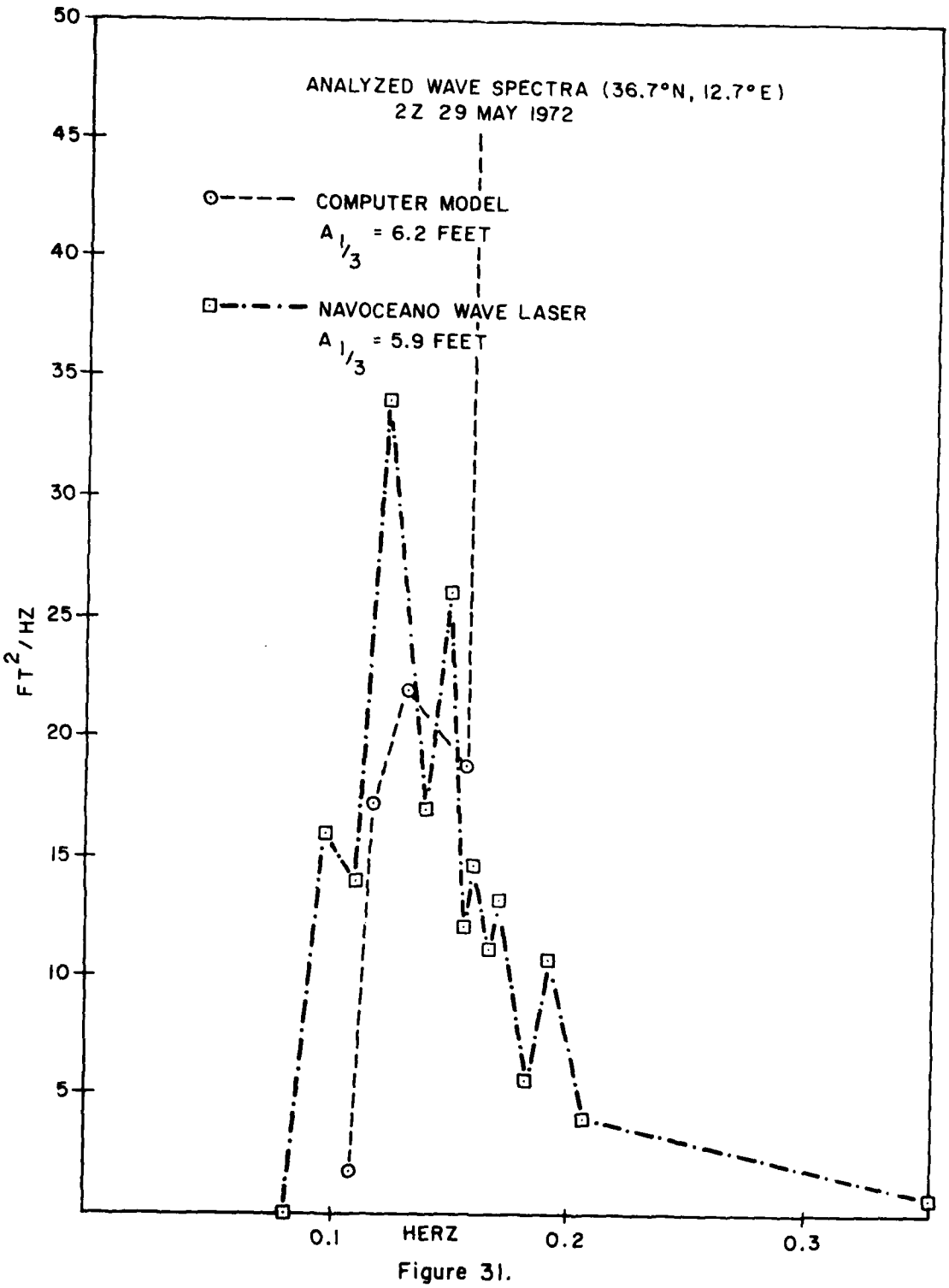
ANALYZED WAVE SPECTRA (36.7°N, 12.7°E)
2Z 29 MAY 1972
COMPUTER MODEL
$A_{1/3}$ = 6.2 FEET
NAVOCEANO WAVE LASER
$A_{1/3}$ = 5.9 FEET
FT²/HZ
50
45
40
35
30
25
20
15
10
5
0.1
HERZ
0.2
0.3

Figure 31.

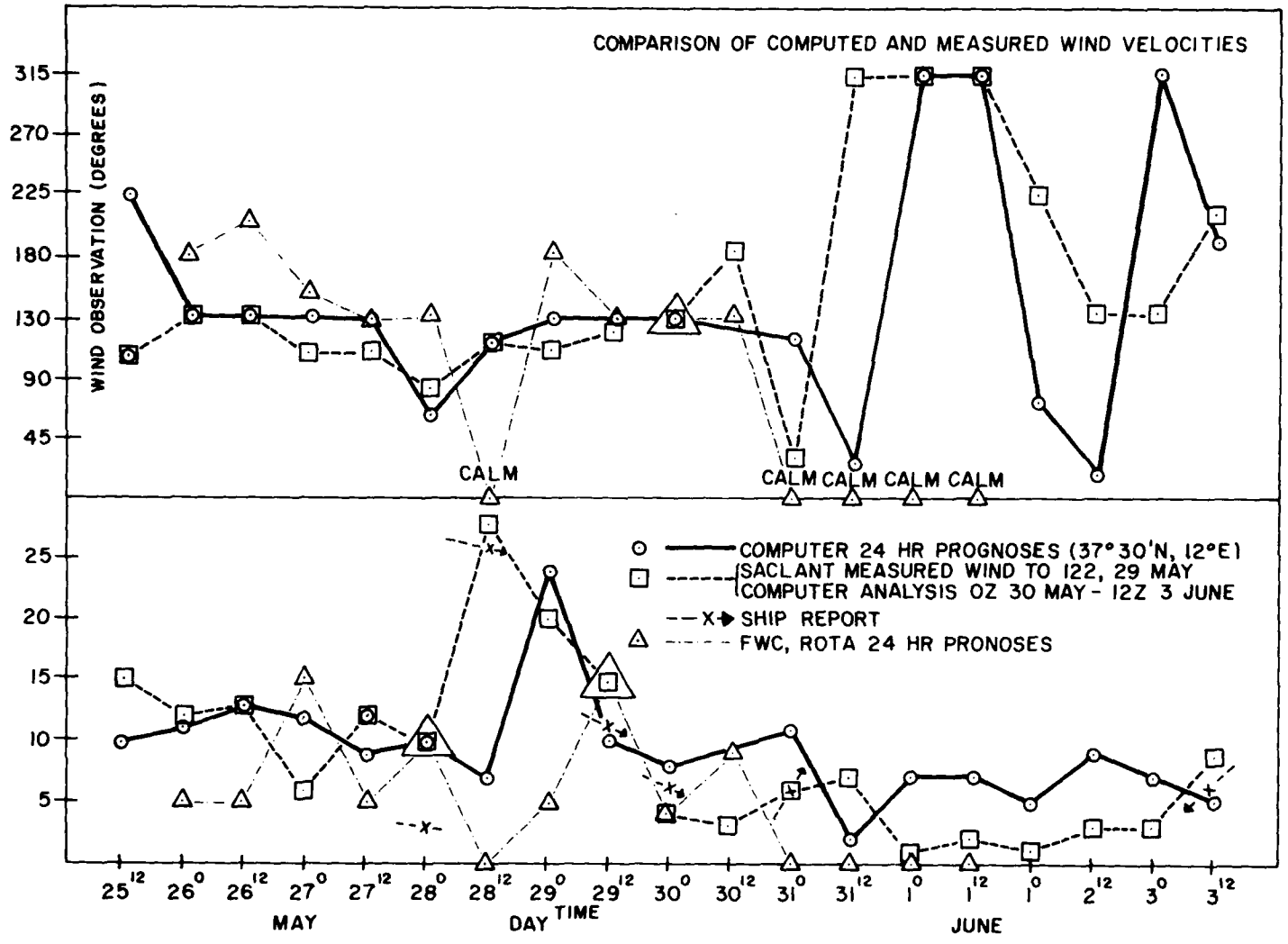
COMPARISON OF COMPUTED AND MEASURED WIND VELOCITIES
WIND OBSERVATION (DEGREES)
315
270
225
180
130
90
45
CALM
CALM CALM CALM CALM
25
20
15
10
5
COMPUTER 24 HR PROGNOSES (37°30'N, 12°E)
SACLANT MEASURED WIND TO 122, 29 MAY
COMPUTER ANALYSIS 0Z 30 MAY - 12Z 3 JUNE
SHIP REPORT
FWC, ROTA 24 HR PRONOSES
25 12 26 0 26 12 27 0 27 12 28 0 28 12 29 0 29 12 30 0 30 12 31 0 31 12 1 0 1 12 1 0 2 12 3 0 3 12
MAY
DAY TIME
JUNE

FIGURE 32

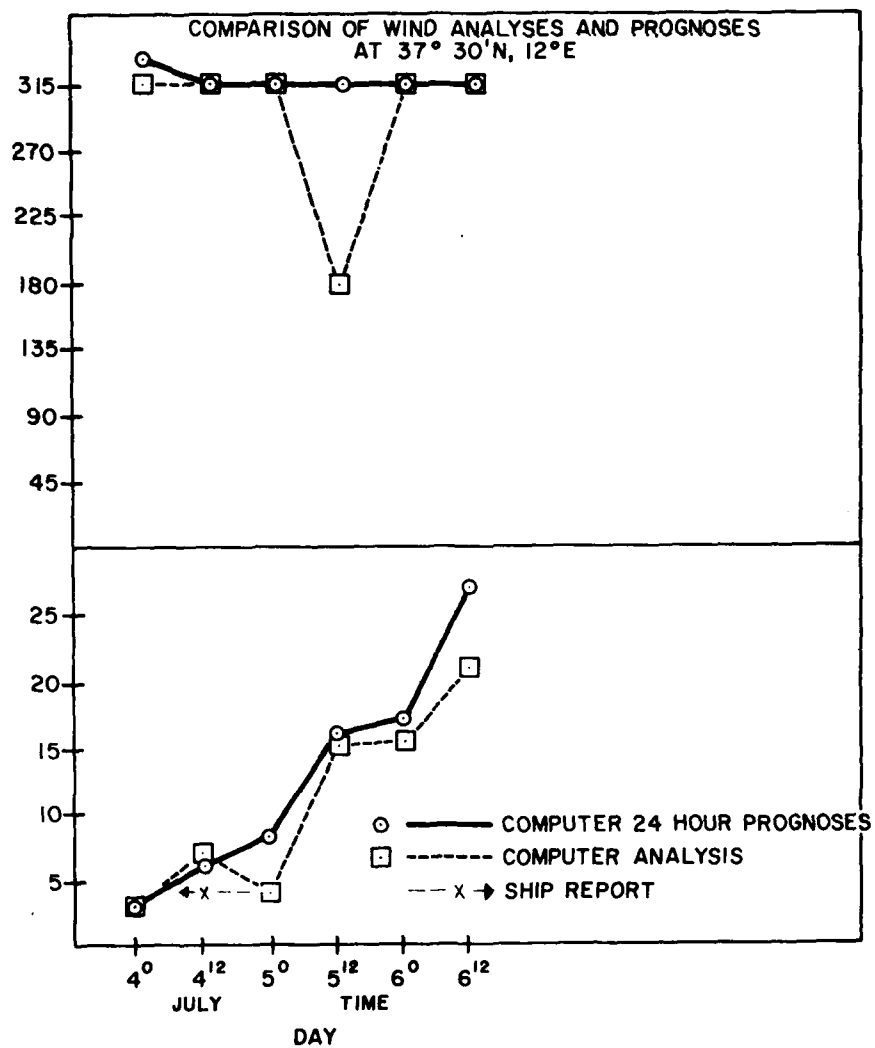
COMPARISON OF WIND ANALYSES AND PROGNOSES
AT 37° 30'N, 12°E
315
270
225
180
135
90
45
25
20
15
10
5
COMPUTER 24 HOUR PROGNOSES
COMPUTER ANALYSIS
SHIP REPORT
4^0
4^12
5^0
5^12
6^0
6^12
JULY
TIME
DAY

FIGURE 33

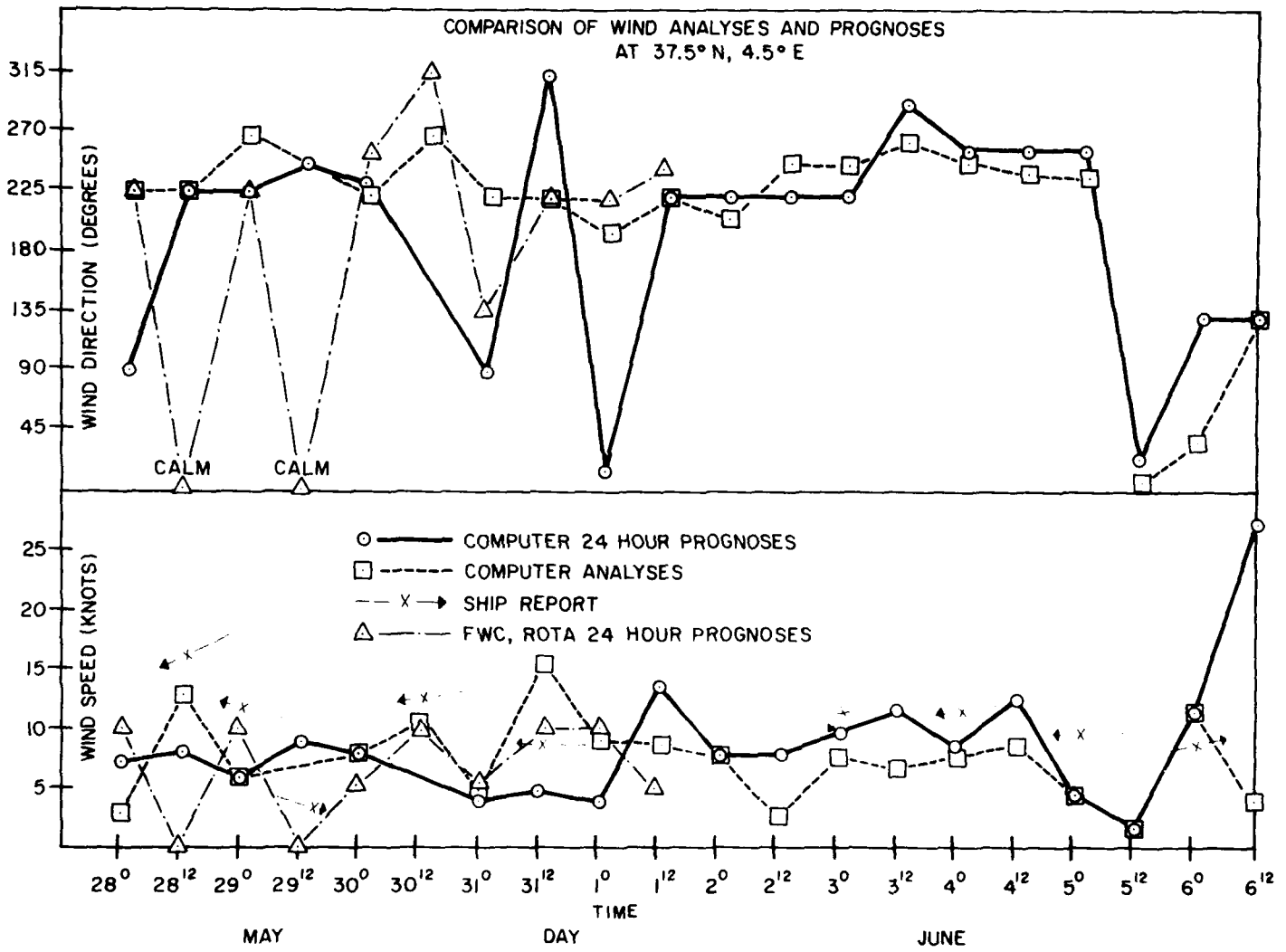
COMPARISON OF WIND ANALYSES AND PROGNOSES
AT 37.5° N, 4.5° E
WIND DIRECTION (DEGREES)
315
270
225
180
135
90
45
CALM
CALM
WIND SPEED (KNOTS)
25
20
15
10
5
COMPUTER 24 HOUR PROGNOSES
COMPUTER ANALYSES
SHIP REPORT
FWC, ROTA 24 HOUR PROGNOSES
28° 28¹² 29° 29¹² 30° 30¹² 31° 31¹² 1° 1¹² 2° 2¹² 3° 3¹² 4° 4¹² 5° 5¹² 6° 6¹²
TIME
MAY
DAY
JUNE

FIGURE 34

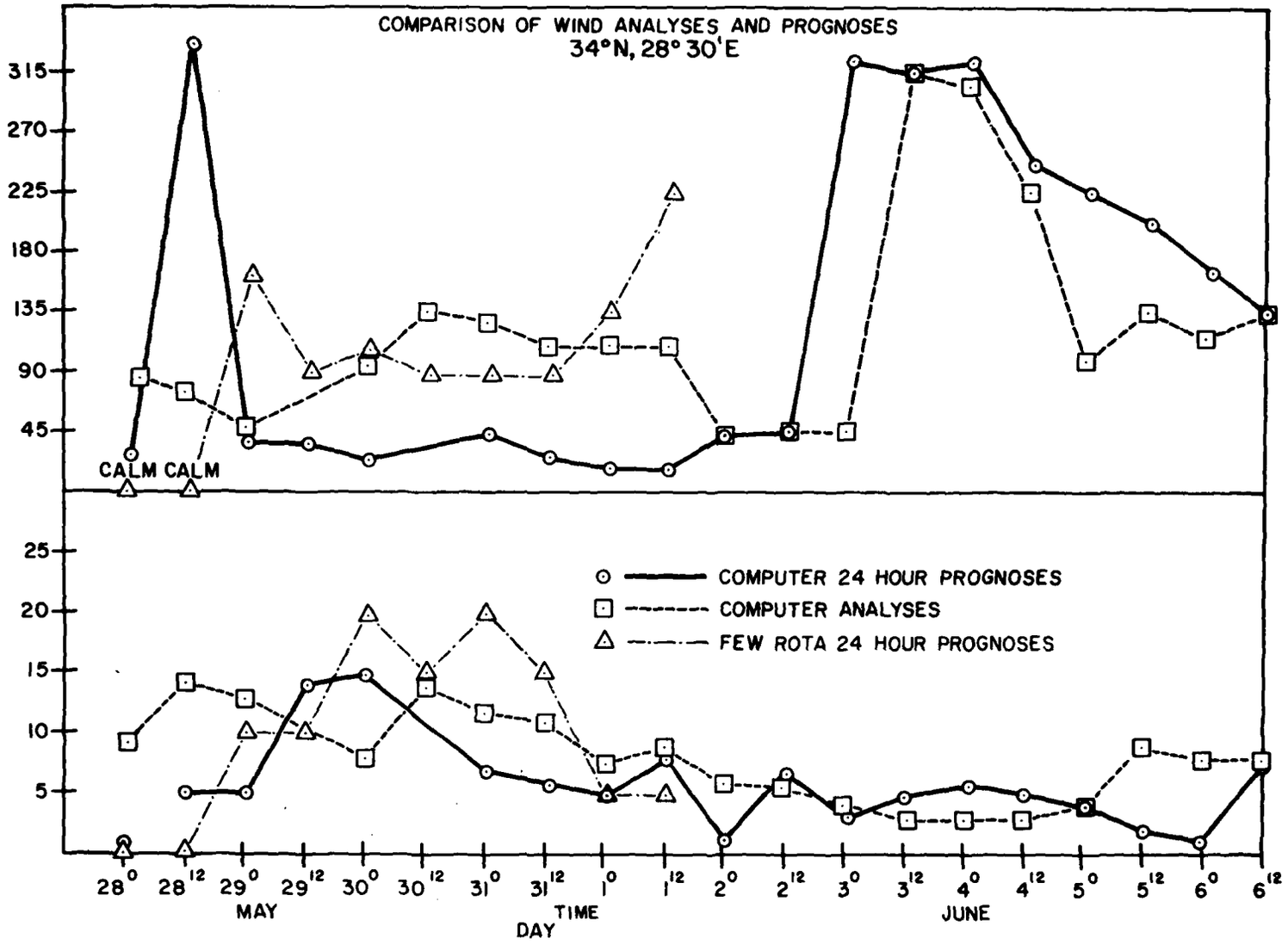
COMPARISON OF WIND ANALYSES AND PROGNOSES
34°N, 28° 30'E
315
270
225
180
135
90
45
CALM CALM
25
20
15
10
5
COMPUTER 24 HOUR PROGNOSES
COMPUTER ANALYSES
FEW ROTA 24 HOUR PROGNOSES
28^0 28^12 29^0 29^12 30^0 30^12 31^0 31^12 1^0 1^12 2^0 2^12 3^0 3^12 4^0 4^12 5^0 5^12 6^0 6^12
MAY
JUNE
DAY
TIME

FIGURE 35

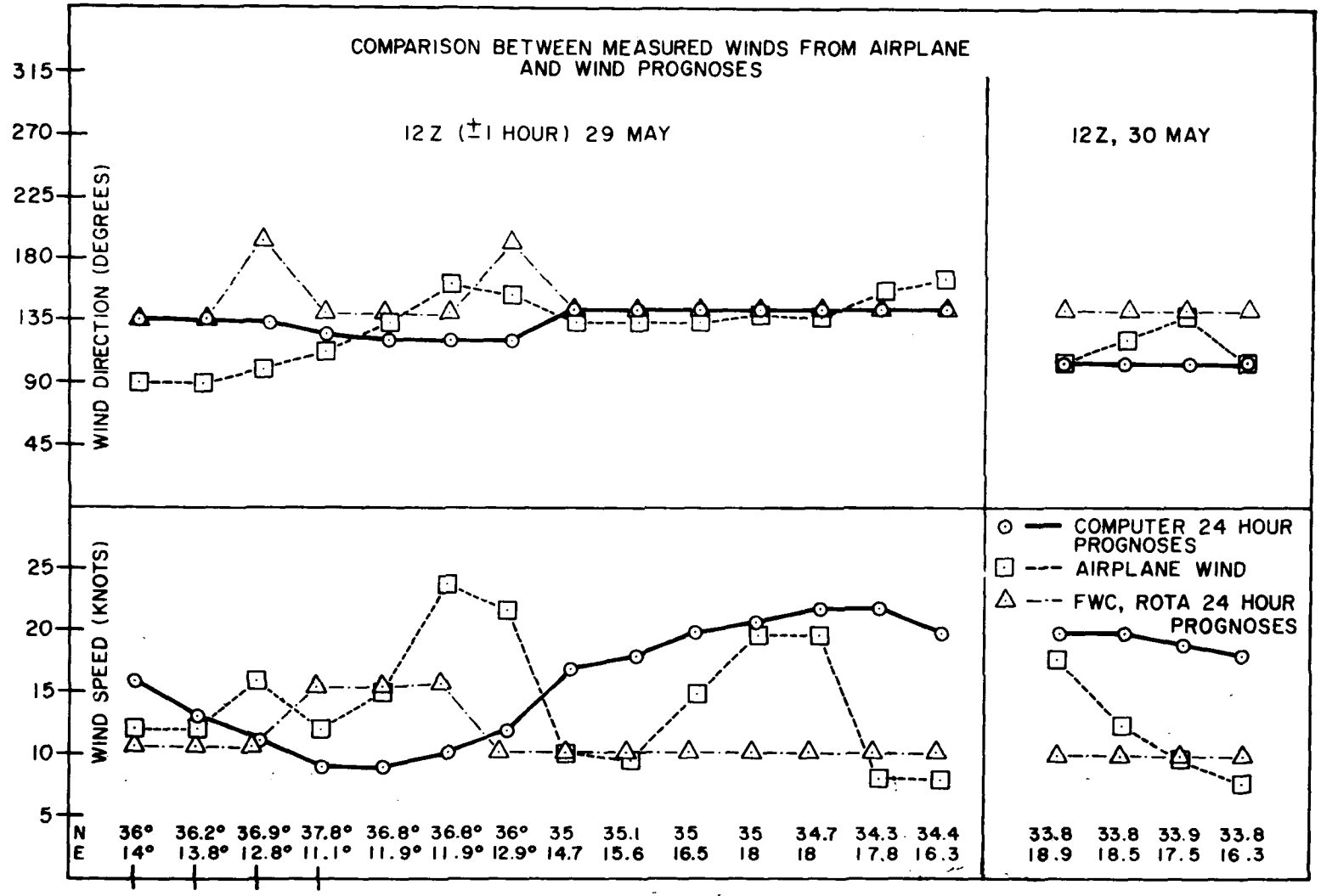
COMPARISON BETWEEN MEASURED WINDS FROM AIRPLANE AND WIND PROGNOSES
12 Z (±1 HOUR) 29 MAY
12Z, 30 MAY
WIND DIRECTION (DEGREES)
315
270
225
180
135
90
45
WIND SPEED (KNOTS)
25
20
15
10
5
COMPUTER 24 HOUR PROGNOSES
AIRPLANE WIND
FWC, ROTA 24 HOUR PROGNOSES
N 36° 36.2° 36.9° 37.8° 36.8° 36.8° 36° 35 35.1 35 35 34.7 34.3 34.4
E 14° 13.8° 12.8° 11.1° 11.9° 11.9° 12.9° 14.7 15.6 16.5 18 18 17.8 16.3
33.8 33.8 33.9 33.8
18.9 18.5 17.5 16.3

FIGURE 36

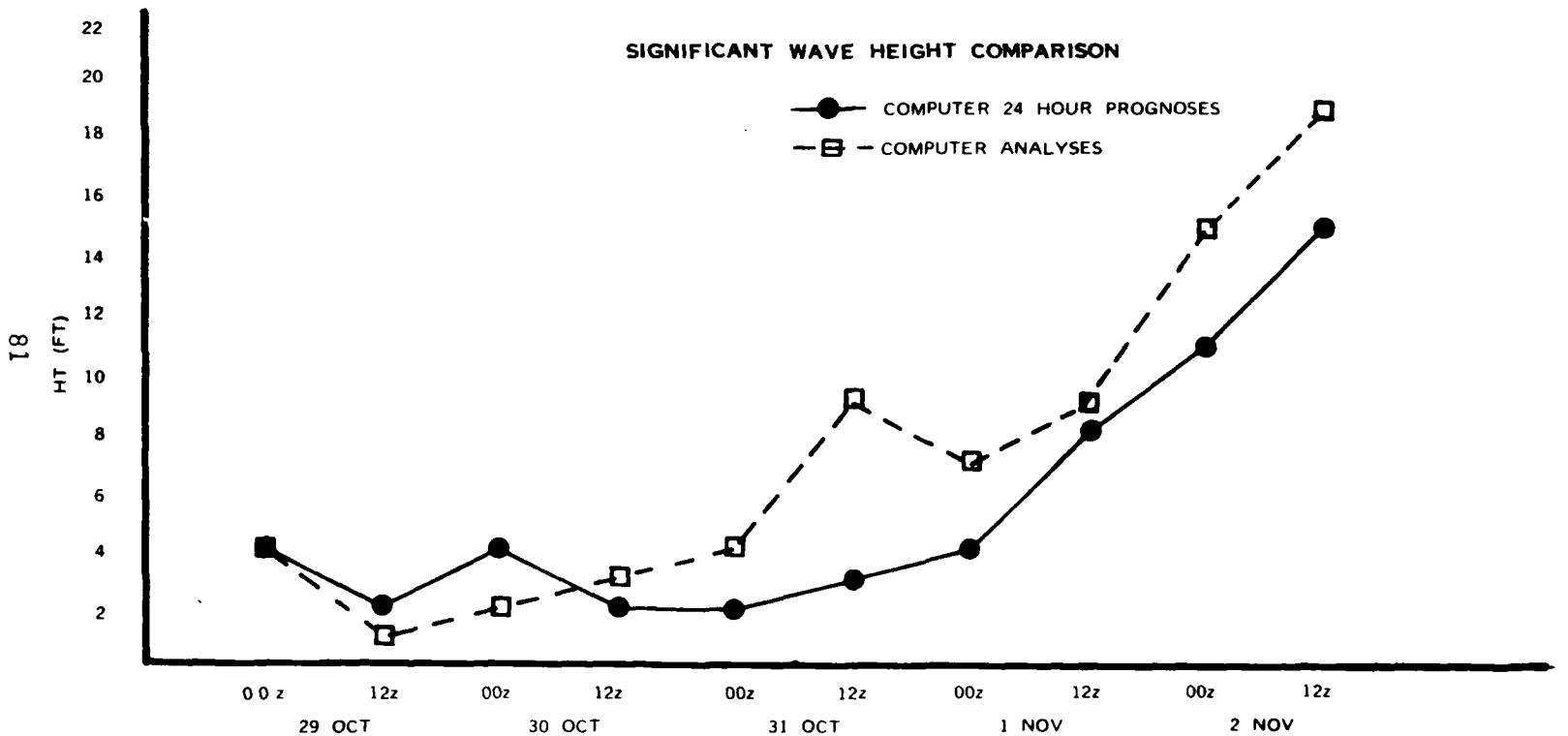
SIGNIFICANT WAVE HEIGHT COMPARISON
COMPUTER 24 HOUR PROGNOSES
COMPUTER ANALYSES
HT (FT)
22
20
18
16
14
12
10
8
6
4
2
00z
12z
00z
12z
00z
12z
00z
12z
00z
12z
29 OCT
30 OCT
31 OCT
1 NOV
2 NOV

FIGURE 37

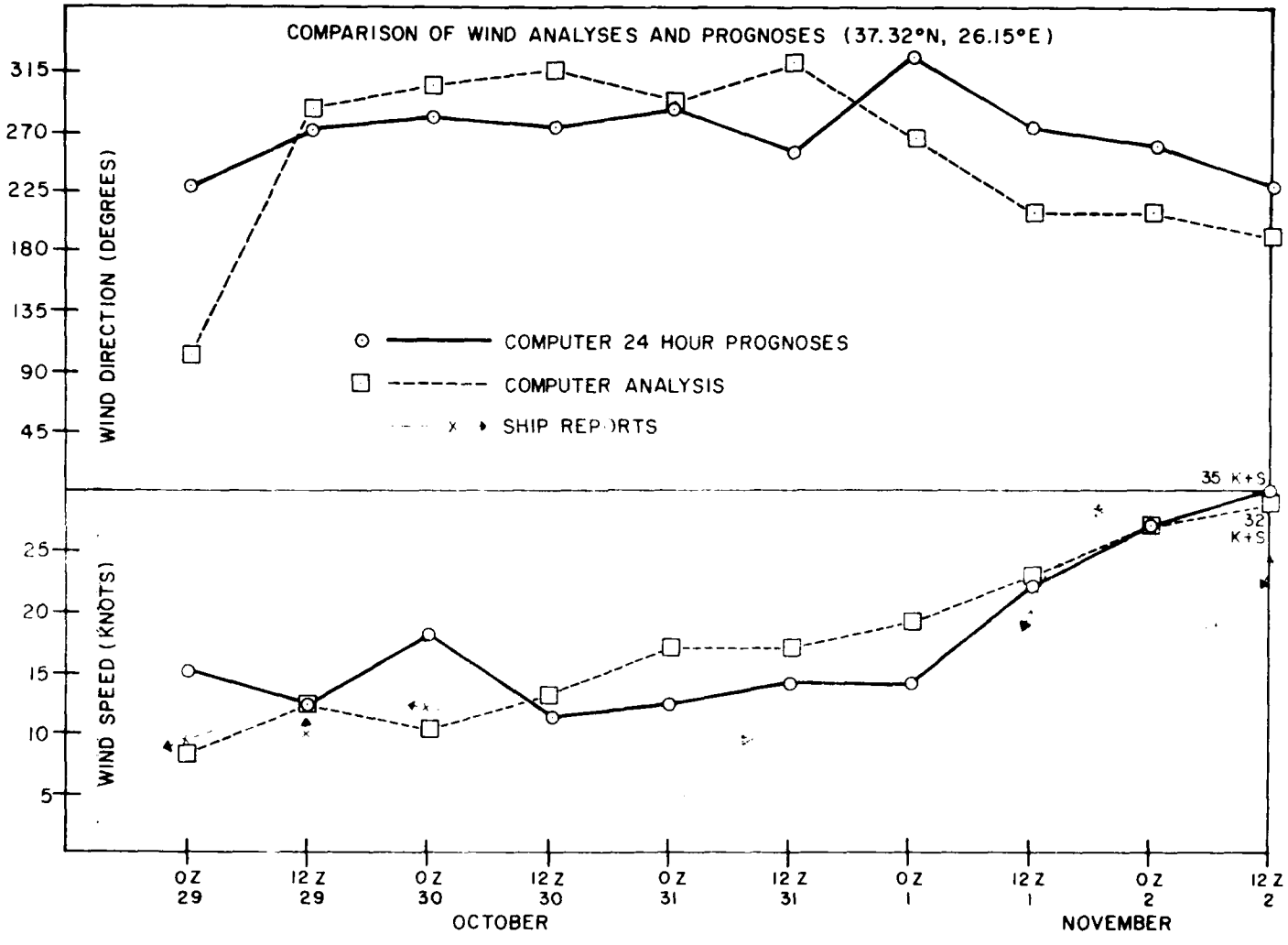
COMPARISON OF WIND ANALYSES AND PROGNOSES (37.32°N, 26.15°E)
WIND DIRECTION (DEGREES)
315
270
225
180
135
90
45
COMPUTER 24 HOUR PROGNOSES
COMPUTER ANALYSIS
SHIP REPORTS
WIND SPEED (KNOTS)
25
20
15
10
5
35 K+S
32 K+S
0Z 29
12Z 29
0Z 30
12Z 30
0Z 31
12Z 31
0Z 1
12Z 1
0Z 2
12Z 2
OCTOBER
NOVEMBER

FIGURE 38

UNCLASSIFIED
Security Classification

DOCUMENT CONTROL DATA - R & D

Security classification of title, body of abstract and indexing annotation must be entered when the overall report is classified)

1. ORIGINATING ACTIVITY (Corporate author)
Fleet Numerical Weather Central

2a. REPORT SECURITY CLASSIFICATION
Unclassified

2b. GROUP

3. REPORT TITLE
(1) A Mediterranean Sea Wave Spectral Model

4. DESCRIPTIVE NOTES (Type of report and inclusive dates)
(9) Technical Note No. 73-1, March 1973

5. AUTHOR(S) (First name, middle initial, last name)
(10) Sheldon M. Lazanoff, Norman M. Stevenson, Vincent J. Cardone

6. REPORT DATE
March 1973

7a. TOTAL NO. OF PAGES
(13) 93

7b. NO. OF REFS
15

8a. CONTRACT OR GRANT NO

b. PROJECT NO
(11) NOOO

c.

d.

9a. ORIGINATOR'S REPORT NUMBER(S)

9b. OTHER REPORT NO(S) (Any other numbers that may be assigned this report)

10. DISTRIBUTION STATEMENT
Approved for public release; distribution unlimited

11. SUPPLEMENTARY NOTES

12. SPONSORING MILITARY ACTIVITY
(14) FNWC-TN-73-1

13. ABSTRACT

An operational Mediterranean wave spectral model has been developed through the cooperative efforts of the U.S. Naval Oceanographic Office (NAVOCEANO), Fleet Numerical Weather Central (FNWC) and New York University (NYU). Since April 1972, the model has been operating in a real-time environment (analyses/prognoses to 48 hours). The model is a modified version of the original NYU North Atlantic wave model and has two main parts: (1) wave energy growth based on a modified version of the Miles-Phillips growth mechanism and dissipation at individual grid points and (2) wave energy propagation frim grid point to grid point. The Mediterranean wave model uses a conic conformal grid, permitting the assumption of equal spacing between grid points. There are 455 sea points with a mesh length of 67 km.

The wave model driving force is a modified version of the FNWC Marine Wind model which has a mesh length of approximately 370 kms. For use in the Mediterranean, the winds are interpolated between Marine Wind field grid points. At analysis/pre-analysis times, wind reports from synoptic ship files are reanalyzed in the Mediterranean wind program so that local wind phenomena, such as 'mistrals,' are included in the wind field.

The Mediterranean wind and wave model was evaluated with ship reports, one wave buoy and an airborne wave laser. The wave computations appear to be as good as the wind input allows.

The on-time analyses and 24-hour forecasts of wave heights are transmitted to Fleet Weather Central, Rota, Spain.

DD FORM 1 NOV 65 1473 (PAGE 1)
S/N 0101-807-6801

UNCLASSIFIED 738670
Security Classification

14 KEY WORDS	LINK A		LINK B		LINK C	
	ROLE	WT	ROLE	WT	ROLE	WT
Mediterranean Sea						
Wave Spectra						
Marine Wind Field						
Operational Spectral Wave Model						
Wave Growth						
Wave Propagation						
Wave Dissipation						
Forecasting						
Prognosis						